

Epigenetic regulator CXXC5 recruits DNA demethylase Tet2 to regulate TLR7/9-elicited IFN response in pDCs

Shixin Ma,^{1,2} Xiaoling Wan,³ Zihou Deng,¹ Lei Shi,¹ Congfang Hao,¹ Zhenyuan Zhou,⁵ Chun Zhou,¹ Yiyuan Fang,³ Jinghua Liu,¹ Jing Yang,¹ Xia Chen,¹ Tiantian Li,¹ Aiping Zang,¹ Shigang Yin,³ Bin Li,¹ Joel Plumas,⁶ Laurence Chaperot,⁶ Xiaoming Zhang,³ Guoliang Xu,⁴ Lubin Jiang,³ Nan Shen,⁵ Sidong Xiong,² Xiaoming Gao,² Yan Zhang,³ and Hui Xiao¹

¹CAS Key Laboratory of Molecular Virology and Immunology, Institut Pasteur of Shanghai; CAS Center for Excellence in Molecular Cell Sciences; University of Chinese Academy of Sciences, Chinese Academy of Sciences, Shanghai 200031, China

²Institute of Biology and Medical Sciences, Soochow University, Soochow, Jiangsu 215006, China

³CAS Key Laboratory of Molecular Virology and Immunology, Institut Pasteur of Shanghai and ⁴State Key Laboratory of Molecular Biology, CAS Excellence Center in Molecular Cell Sciences, Institute of Biochemistry and Cell Biology, Shanghai Institutes for Biological Sciences, Chinese Academy of Sciences, Shanghai 200031, China

⁵Shanghai Institute of Rheumatology, Renji Hospital, Shanghai Jiao Tong University School of Medicine, Shanghai 200240, China

⁶Institute for Advanced Biosciences (IAB), Team Immunobiology and Immunotherapy in Chronic Diseases, Institut National de la Santé et de la Recherche Médicale U1209, Centre National de la Recherche Scientifique UMR5309, Université Grenoble Alpes, Etablissement Français du Sang-Rhône-Alpes, F-38700 Grenoble, France

TLR7/9 signals are capable of mounting massive interferon (IFN) response in plasmacytoid dendritic cells (pDCs) immediately after viral infection, yet the involvement of epigenetic regulation in this process has not been documented. Here, we report that zinc finger CXXC family epigenetic regulator CXXC5 is highly expressed in pDCs, where it plays a crucial role in TLR7/9- and virus-induced IFN response. Notably, genetic ablation of CXXC5 resulted in aberrant methylation of the CpG-containing island (CGI) within the *Irf7* gene and impaired IRF7 expression in steady-state pDCs. Mechanistically, CXXC5 is responsible for the recruitment of DNA demethylase Tet2 to maintain the hypomethylation of a subset of CGIs, a process coincident with active histone modifications and constitutive transcription of these CGI-containing genes. Consequently, CXXC5-deficient mice had compromised early IFN response and became highly vulnerable to infection by herpes simplex virus and vesicular stomatitis virus. Together, our results identify CXXC5 as a novel epigenetic regulator for pDC-mediated antiviral response.

INTRODUCTION

By detecting the presence of foreign nucleic acids, plasmacytoid DCs (pDCs) play crucial roles in the induction of both innate and adaptive immune responses (Reizis et al., 2011a; Lewis and Reizis, 2012; Merad et al., 2013; Karrich et al., 2014; Mildner and Jung, 2014; Swiecki and Colonna, 2015). Despite their rare presence in the lymphoid organs and circulating blood, pDCs are superior IFN α producers and immediate responders to viral infection (Reizis et al., 2011b; Ng et al., 2013; Swiecki and Colonna, 2015; Webster et al., 2016). After pDC depletion, the early IFN response to both DNA viruses (HSV, mouse hepatitis virus, and murine CMV) and RNA viruses (vesicular stomatitis virus [VSV] and respiratory syncytial virus) was severely impaired (Lund et al., 2006; Smit et al., 2006; Swiecki et al., 2010, 2013; Takagi et al., 2011; Cervantes-Barragan et al., 2012). Moreover, the pDC-induced IFN response has been shown to be critically involved in the induction of T cell response required for controlling chronic infection by lymphocytic choriomeningitis virus (Blasius et al., 2012; Cervantes-Barragan et al., 2012). In this regard,

pDC depletion or dysfunction has been linked to a variety of human chronic infections, especially the infections caused by HIV (Chehimi et al., 2002; Li et al., 2014; Zhang et al., 2015b), hepatitis B virus (Duan et al., 2004), and hepatitis C virus (Decalf et al., 2007). In addition to viral nucleic acids, pDCs can recognize self-DNAs/RNAs released by necrotic cells, and thus have been implicated in the pathogenesis of autoimmune diseases including systemic lupus erythematosus and psoriasis (Lande et al., 2007; Ganguly et al., 2009, 2013; Rowland et al., 2014; Sisirak et al., 2014). However, how pDCs are genetically and epigenetically programmed for IFN response remains incompletely understood.

Compared with other immune cells, the most remarkable feature of pDCs rests in their unique expression of endosomal sensors TLR7/9 and massive IFN-producing capacity. Unlike TLR3/4 signals, which depend on transcriptional factor IRF3 to induce IFN response, TLR7/9 signals activate IRF7, as well as transcriptional factors NF κ B and AP-1, to elicit IFN α / β production (Kawai et al., 2004). Interestingly, it seems that IRF7 has a more fundamental role than IRF3

Correspondence to Hui Xiao: huixiao@ips.ac.cn

Abbreviations used: 5hmC, 5-methyl-cytosine; cDC, conventional DC; CGI, CpG-containing island; ChIP, chromatin immunoprecipitation; pDC, plasmacytoid DC; pol II, polymerase II; qPCR, quantitative real-time PCR; VSV, vesicular stomatitis virus.

© 2017 Ma et al. This article is distributed under the terms of an Attribution-Noncommercial-Share Alike-No Mirror Sites license for the first six months after the publication date (see <http://www.rupress.org/terms/>). After six months it is available under a Creative Commons License (Attribution-Noncommercial-Share Alike 4.0 International license, as described at <https://creativecommons.org/licenses/by-nc-sa/4.0/>).



in mounting IFN response to a broad spectrum of viruses (Honda et al., 2005), and IRF7 deficiency can lead to recurrent influenza infection in humans (Ciancanelli et al., 2015). Although most cells express IRF7 only after viral infection through feedback IFN α / β signaling, pDCs are capable of expressing IRF7 in the steady state (Sato et al., 2000; Izaguirre et al., 2003; Ning et al., 2011). Because both pDCs and IRF7 play such a pivotal role in IFN response, how pDCs manage to express IRF7 constitutively needs to be precisely defined. Indeed, some recent findings have begun to shed light on this issue. Transcriptional factors E2-2 and STAT3 not only are essential for pDC development and maintenance, but also are critically involved in IRF7 expression in the steady state (Laouar et al., 2003; Ghosh et al., 2010; Li et al., 2012). Conversely, DNA methylation of CpG-containing island (CGI) encompassing *Irf7* promoter has been shown to be involved in silencing *Irf7* expression in human fibroblasts (Lu et al., 2000). However, whether this layer of epigenetic regulation also operates in immune cells remains uncharacterized.

CpG islands enriched for CpG dinucleotides are present in ~70% of mammalian gene promoters. Not surprisingly, CGIs can profoundly shape chromatin structure, thereby participating in the regulation of gene expression. Although CpG islands are frequently hypomethylated or unmethylated in somatic cells, and mostly associated with active gene transcription, mounting evidence suggests that CGIs can become hypermethylated in certain immune cells, and more frequently in malignant cells, leading to gene silencing instead (Blackledge and Klose, 2011; Li and Zhang, 2014; Smale et al., 2014; Ko et al., 2015). Recent identification and elucidation of zinc finger CXXC proteins (ZF-CXXC proteins) have provided better understanding of the dynamic nature of CGIs and their intricate link with histone modifications (Long et al., 2013). Despite their conserved function in recognizing unmethylated CpGs, ZF-CXXC proteins are very much diversified structurally and functionally. Although DNA methyltransferase Dnm1 and DNA dioxygenase Tet1/3 are involved in DNA methylation (Gu et al., 2011; Li and Zhang, 2014), histone methyltransferases Mll1/2, histone demethylases Kdm2a/b, and Cfp1 mainly participate in the regulation of histone methylation (Farcas et al., 2012; Blackledge et al., 2013). Conversely, CXXC5 and its close homologue CXXC4 do not possess any enzymatic activity, and their physiological functions have just begun to unfold (Long et al., 2013). Recent findings imply that CXXC5 can be involved in a variety of physiological processes including myelopoiesis, osteopoiesis, and neural cell development (Pendino et al., 2009; Kim et al., 2015, 2016) and also takes part in DNA damage response, skin repair, and hematological malignancy (Pendino et al., 2009; Zhang et al., 2009; Lee et al., 2015). In these processes, CXXC5 primarily acts as a signaling component regulating ATM-p53 or wnt- β -catenin pathways (Andersson et al., 2009; Zhang et al., 2009; Kim et al., 2010, 2015; Lee et al., 2015). Recently, CXXC5 has been reported to be associated with epigenetic regulators Tet2 and

SUV39H1 (Ko et al., 2013; Tsuchiya et al., 2016), implying a possible role for CXXC5 in epigenetic regulation of gene expression. In this study, we provide compelling evidence supporting a crucial role for CXXC5 in the regulation of DNA methylation and IFN response in pDCs, thereby demonstrating an additional layer of regulation integral to pDC function and antiviral defense.

RESULTS

CXXC5 plays a critical role in pDC-elicited IFN response

In the past decade, resources generated by immune cell gene profiling have led to the identification of lineage-specific regulators and the elucidation of principles governing immune cell specification. By searching these databases, we found that the putative epigenetic regulator CXXC5 is preferentially expressed in human and mouse pDCs (Robbins et al., 2008; Ghosh et al., 2010; Miller et al., 2012). Moreover, CXXC5, along with MAVS/IPS-1/VISA, has been previously linked to IFN response through a cDNA library screening (Kawai et al., 2005). These clues prompted us to investigate the role of CXXC5 in pDCs.

By quantitative real-time PCR (qPCR) and Western blotting, we confirmed that CXXC5 is expressed predominantly in pDCs, much less in lymphocytes, and barely detectably in conventional DCs (cDCs) or macrophages (Fig. 1, A and B). Next, we generated CXXC5-deficient mice by conventional gene-targeting strategy on 129/Ola strain (Fig. S1, A and B), and then backcrossed onto C57/B6 background for six generations. By Western blotting, we confirmed that CXXC5 expression was completely lost in various organs of CXXC5^{-/-} mice, especially in the spleen and thymus (Fig. S1 C). By flow cytometry analyses, we found that the percentage and number of pDCs and cDCs in CXXC5^{-/-} spleens were comparable to those in WT controls (Fig. 1 C). Moreover, B and T lymphocytes, neutrophils, and monocytes were normally generated in CXXC5^{-/-} mice (Fig. S1, D and E).

Because CXXC5 does not appear to affect pDC development, we went on to investigate its involvement in pDC function, especially in antiviral IFN response. We first isolated pDCs from WT and CXXC5^{-/-} spleens by FACS and stimulated them ex vivo with HSV-1, a DNA virus known to engage TLR9 on pDCs, for 24 h. By ELISA, we detected large amounts of IFN α and IFN β secreted by WT pDCs after HSV-1 stimulation; however, the induction of IFN α / β by HSV-1 was diminished in CXXC5^{-/-} pDCs (Fig. 1 D). Next, we infected both WT and CXXC5^{-/-} mice with HSV-1 i.v. for 9 h and then purified splenic pDCs by FACS sorting (Fig. S1 F). Real-time PCR analyses demonstrated that the induction of *Irfn4* and *Irfn3* mRNAs by in vivo HSV-1 infection was severely impaired in CXXC5^{-/-} pDCs (Fig. 1 E). Furthermore, after i.v. injection of A-type CpG DNAs (CpG-A, mainly engages TLR9 on pDCs) complexed with liposome DOTAP, CXXC5^{-/-} mice also exhibited attenuated IFN α response (Fig. 1 F). Together, these results uncovered a novel role for CXXC5 in pDC-elicited IFN response to viral infection.

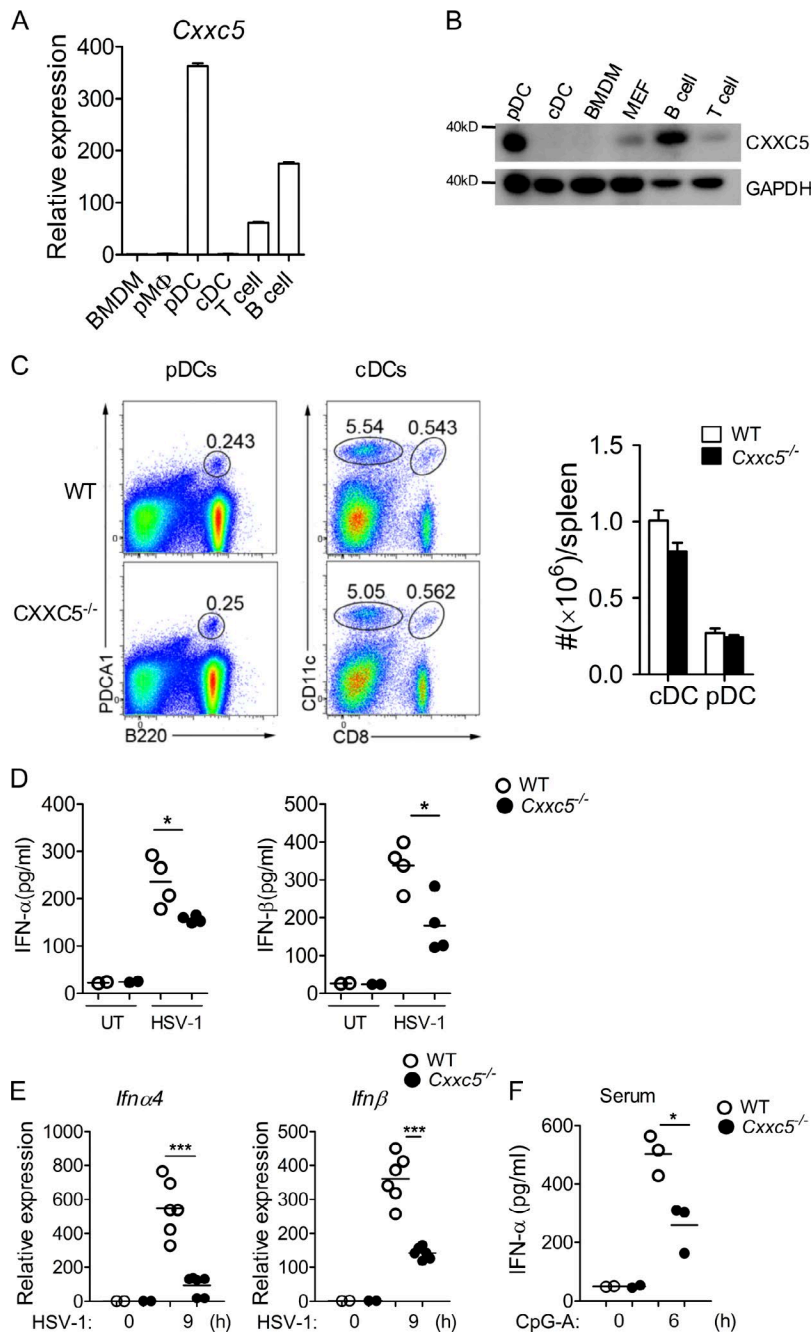


Figure 1. Expression and function of CXXC5 in pDCs.

(A) Total mRNAs were extracted from BMDMs, thioglycolate-elicited peritoneal macrophages, Flt3L-differentiated pDCs, GM-CSF-differentiated BMDCs (cDCs), and splenic T and B cells isolated by anti-CD3 or anti-CD19 microbeads, respectively. The relative expression of *Cxyc5* over *Gapdh* was measured by real-time PCR, and the data are presented as mean \pm SD. This experiment was conducted twice with similar results. (B) Whole-cell lysates were prepared from Flt3L-pDCs, GM-CSF-cDCs, BMDMs, MEFs, splenic T cells, and B cells, and Western blotting was conducted with anti-CXXC5 antibody. This experiment was conducted twice with similar results. (C) Percentage of cDCs (CD11c^{hi}, gated on B220⁻CD3⁻ cells) and pDCs (B220⁺PDCA1⁺CD11c^{int}) in spleens was analyzed by flow cytometry, and total numbers of cDCs and pDCs were counted. This experiment was repeated three times, and similar results were obtained. The data are presented as mean \pm SD. (D) Splenic pDCs (10⁶ cells/ml) purified from WT and CXXC5^{-/-} mice ($n = 4$) were infected with HSV-1 for 24 h. Production of IFN α/β was measured by ELISA. This experiment was repeated twice, and representative data (mean \pm SD) are shown (*, $P < 0.05$, analyzed by Student's *t* test). (E) WT and CXXC5^{-/-} mice ($n = 6$) were either uninfected or i.v. infected with HSV-1 (5 \times 10⁶ pfu/mouse) for 9 h, and splenocytes were sorted by FACS. Total mRNA was prepared from 10⁵ pDCs (CD11c^{int}B220⁺/PDCA1⁺/Siglec-H^{hi}) and quantified by real-time PCR. This experiment was repeated twice, and representative data are shown (***, $P < 0.001$, analyzed by Student's *t* test). (F) WT and CXXC5^{-/-} mice ($n = 3$) were either untreated or treated with i.v. injection of 20 μ g CpG-A (complexed with 30 μ g DOTAP) for 6 h, and sera were collected for ELISA. This experiment was performed three times with similar results (*, $P < 0.05$, analyzed by Student's *t* test).

CXXC5 regulates TLR7/9-induced IFN response in pDCs

pDCs are rarely present in vivo and account for <0.5% of total spleen cells. Alternatively, in vitro pDCs generated from BM by cytokine Flt3L closely resemble in vivo pDCs and have been widely used for studies on IFN response. Subsequently, we used in vitro pDCs (CD11c^{int}B220⁺CD11b⁻) sorted from Flt3L-differentiated BMDCs (Flt3L-BMDCs) by FACS for the following experiments. After stimulation by HSV-1 for 24 h, Flt3L-pDCs recapitulated splenic pDCs with abundant IFN α/β production (Fig. 2 A). Similarly, CXXC5^{-/-} pDCs produced much less IFN α/β than

WT pDCs after stimulation by HSV-1 or CpG-A (Fig. 2, A and B). Concomitantly, the induction of chemokine CCL-5, as well as cytokines TNF and IL-12, was also dampened in CXXC5^{-/-} pDCs (Fig. 2, A and B).

Although TLR9 is involved in the recognition of viral DNAs in pDCs, TLR7 is a designated sensor for viral single-stranded RNAs. After stimulation by RNA virus VSV, the induction of IFN α/β , CCL-5, TNF, and IL-12 was universally attenuated in CXXC5^{-/-} pDCs (Fig. 2 C). Moreover, CXXC5^{-/-} pDCs also produced less IFN α/β , CCL-5, TNF, and IL-12 than WT pDCs after stimulation by TLR7 ligand

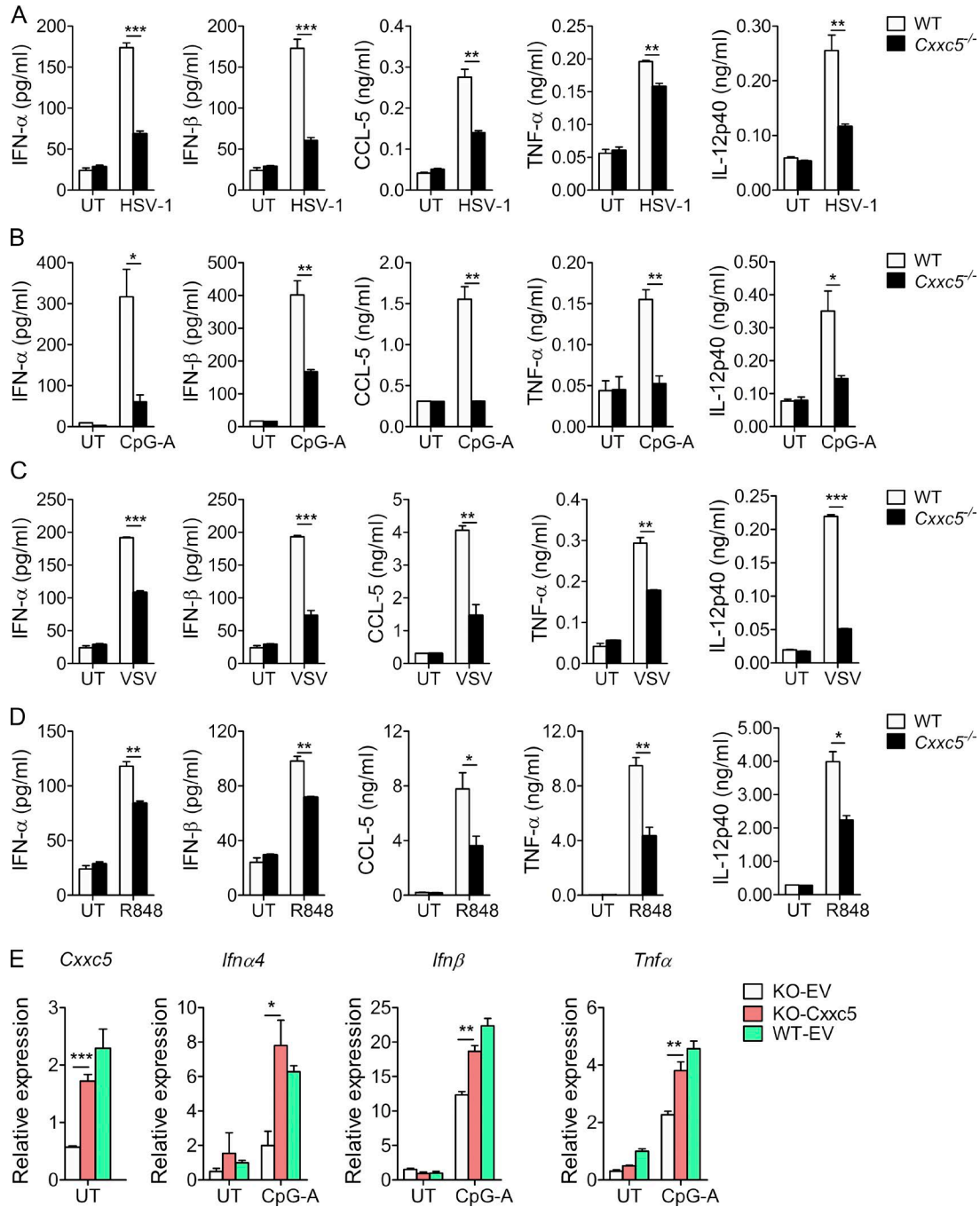


Figure 2. **Virus- and TLR7/9-induced gene expression in WT and CXXC5^{-/-} pDCs.** (A–D) 2 × 10⁵ Flt3L-differentiated BM-derived pDCs (CD11c^{int}-B220⁺CD11b⁻) sorted by FACS were either untreated (UT) or treated with HSV-1 (MOI: 1; A), CpG-A (2 μg/ml; B), VSV (MOI: 1; C), or R848 (1 μg/ml; D) for 24 h, and the supernatants (n = 3) were collected for ELISA. These experiments were conducted three times, and representative data (mean ± SD) are shown (*, P < 0.05; **, P < 0.01; ***, P < 0.001, analyzed by Student's *t* test). (E) WT and CXXC5^{-/-} (KO) Flt3L-pDCs transduced by lentiviral vector or CXXC5-expressing lentiviruses were sorted as GFP-positive cells by FACS and treated with CpG-A (2 μg/ml) for 6 h. Expression levels of *Ifna*/*β* and *Tnfα* mRNAs were quantified by real-time PCR, and the data are presented as mean ± SD. This experiment was repeated twice with similar results (*, P < 0.05; **, P < 0.01; ***, P < 0.001, analyzed by Student's *t* test).

R848 (Fig. 2 D). Subsequently, we sought to test whether restoring CXXC5 expression in CXXC5^{-/-} pDCs could rescue the defective IFN response. To this end, we reexpressed CXXC5 in CXXC5^{-/-} pDCs by lentiviral vector-mediated transduction. Notably, restored CXXC5 expression largely rescued the defective IFN response exhibited by CXXC5^{-/-} pDCs, as they now produced levels of *Ifna4*, *Ifnb*, and *Tnf* comparable with WT pDCs in response to CpG-A stimulation (Fig. 2 E). Collectively, these results demonstrated that CXXC5 has a crucial role in TLR7/9-induced IFN response.

CXXC5 regulates TLR-induced responses in a cell type-specific manner

Unlike CpG-A, which specifically operates in pDCs, B-type CpG DNAs (CpG-B) can trigger a TLR9-dependent proinflammatory response in a diversity of immune cells including pDCs, cDCs, macrophages, and B cells. After CpG-B stimulation, CXXC5^{-/-} pDCs produced less TNF and IL-6 than WT pDCs (Fig. 3 A). Moreover, CpG-B-induced TNF and IL-6 were also decreased in CXXC5^{-/-} B cells (Fig. 3 B), further supporting a positive role for CXXC5 in TLR9 signaling. However, in CpG-B-stimulated BMDCs (GM-CSF-differentiated BMDCs) and BMDMs, CXXC5 deficiency did not affect the induction of TNF or IL-6 (Fig. 3, C and D), underscoring a cell type-specific role for CXXC5 in TLR9 signaling. Similarly, although CXXC5 deficiency resulted in attenuated TNF and IL-6 expression in B cells upon LPS stimulation (Fig. 3 E), LPS-induced IFN type I and proinflammatory responses were largely intact in CXXC5^{-/-} BMDCs (Fig. 3 F). Therefore, although CXXC5 is involved in a broad range of TLR signals featured by TLR4, TLR7, and TLR9, it only operates in a narrow spectrum of immune cells, particularly in pDCs and B cells that express large amounts of CXXC5 proteins (Fig. 1 B).

To determine how CXXC5 regulates the TLR9-induced proinflammatory response, we examined CpG-B-induced signaling events. Surprisingly, similar levels of p-IKK α / β , p-IkBa, p-p38, and p-ERK were detected in WT and CXXC5^{-/-} pDCs after CpG-B stimulation (Fig. 3 G), indicating that CXXC5 does not seem directly affect the activation of NFkB or MAPKs in TLR9 signaling. On the other hand, we found that CXXC5 deficiency influenced the recruitment of p65 NFkB to proinflammatory genes (Fig. 3, H and I). First, by chromatin immunoprecipitation (ChIP)-qPCR analyses, we detected attenuated p65 binding to the promoters of several proinflammatory genes, such as *Il6*, *Cxcl2*, and *Ccl5*, in CXXC5^{-/-} pDCs after CpG-B stimulation (Fig. 3 H). Second, the enrichment of p65 to the promoters of *Tnf* and *IL-6* was also diminished in CXXC5^{-/-} B cells stimulated by either CpG-B or LPS (Fig. 3 I). Together, these data implied that CXXC5 might impinge on NFkB recruitment to influence proinflammatory gene expression.

CXXC5 regulates IRF7 in TLR9-induced IFN response

In contrast to CpG-B, CpG-A stimulation leads to the activation of IRF7 in pDCs through IKK α (Hoshino et al., 2006)

and mTOR (Cao et al., 2008), which then collaborate with IKK β and MAPKs to induce an IFN response. By Western blotting, we found that CpG-A-induced phosphorylation and degradation of IkB α were comparable between WT and CXXC5^{-/-} pDCs (Fig. 4 A). Further, the phosphorylation of p38, mTOR, and S6 was similarly induced by CpG-A in both WT and CXXC5^{-/-} pDCs (Fig. 4 A). Overall, CXXC5 deficiency did not compromise CpG-A-induced activation of NFkB, MAPKs, and mTOR in pDCs. In contrast, we found that IRF7, but not IRF8, proteins were decreased in CXXC5^{-/-} pDCs that were either untreated or treated with CpG-A (Fig. 4 B). Consistently, the phosphorylation of STAT1 was also impaired in CXXC5^{-/-} pDCs (Fig. 4 B), likely because of decreased IFN response in these cells (Fig. 2 B). Intriguingly, the levels of CXXC5 protein and mRNA gradually declined after CpG-A stimulation (Fig. 4, B and C), a phenomenon also observed in human pDCs (Fig. 4 D). Moreover, *Cxxc5* expression was also down-regulated by IFN β stimulation (Fig. 4 C), implying feedback regulation on CXXC5 expression in pDCs. Given the down-regulation of E2-2 upon pDC activation (Ghosh et al., 2010), it is tempting to propose that these feedback mechanisms may be required to control the duration of TLR9 signaling in pDCs.

Next, we assessed the activation of IRF7 by CpG-A signal through immunofluorescence and ChIP analyses. Although IRF7 primarily resided in the cytoplasm of untreated pDCs, activated IRF7 was translocated to the nuclei after CpG-A stimulation (Fig. 4 E). Notably, compared with WT pDCs, fewer nuclear IRF7 proteins were induced by CpG-A in CXXC5^{-/-} pDCs (Fig. 4 E). Furthermore, IRF7 binding to the promoters of *Ifna4* and *Ifnb* was also lessened in CpG-A-treated CXXC5^{-/-} pDCs (Fig. 4 F). Concomitantly, epigenetic markers associated with active transcription (such as H3K4me3, H3K27ac, and H4ac) were decreased on *Ifna4* promoter of CXXC5^{-/-} pDCs (Fig. 4 G). Therefore, CXXC5 appears to play a role in the recruitment of IRF7 to *Ifna4*/ β genes.

CXXC5 regulates the methylation of CpG islands in pDCs

Next, we conducted global gene expression profiling to gain comprehensive understanding of CXXC5-regulated genes in both steady-state and activated pDCs (Fig. 5 A and Table S1). Notably, among CpG-A-induced genes that were down-regulated by CXXC5 deficiency (>1.5-fold), *Ifna*/ β / λ members were highly enriched (Fig. 5 A). Remarkably, another group of genes that were down-regulated in both steady-state and CpG-A-activated CXXC5^{-/-} pDCs were CGI-containing genes, such as *Irf7*, *Fos*, *Cxcl2*, and *Tnf* (Fig. 5 A). The third group is composed of genes encoding cytokines and chemokines whose expression was neither driven by IRF7 nor regulated by CGI (Fig. 5 A). These data suggested an interesting scenario, that CXXC5 may be primarily involved in the regulation of CGI-containing genes, whose products (such as IRF7) then contribute to rapid and robust IFN response in pDCs. To this end, we validated that

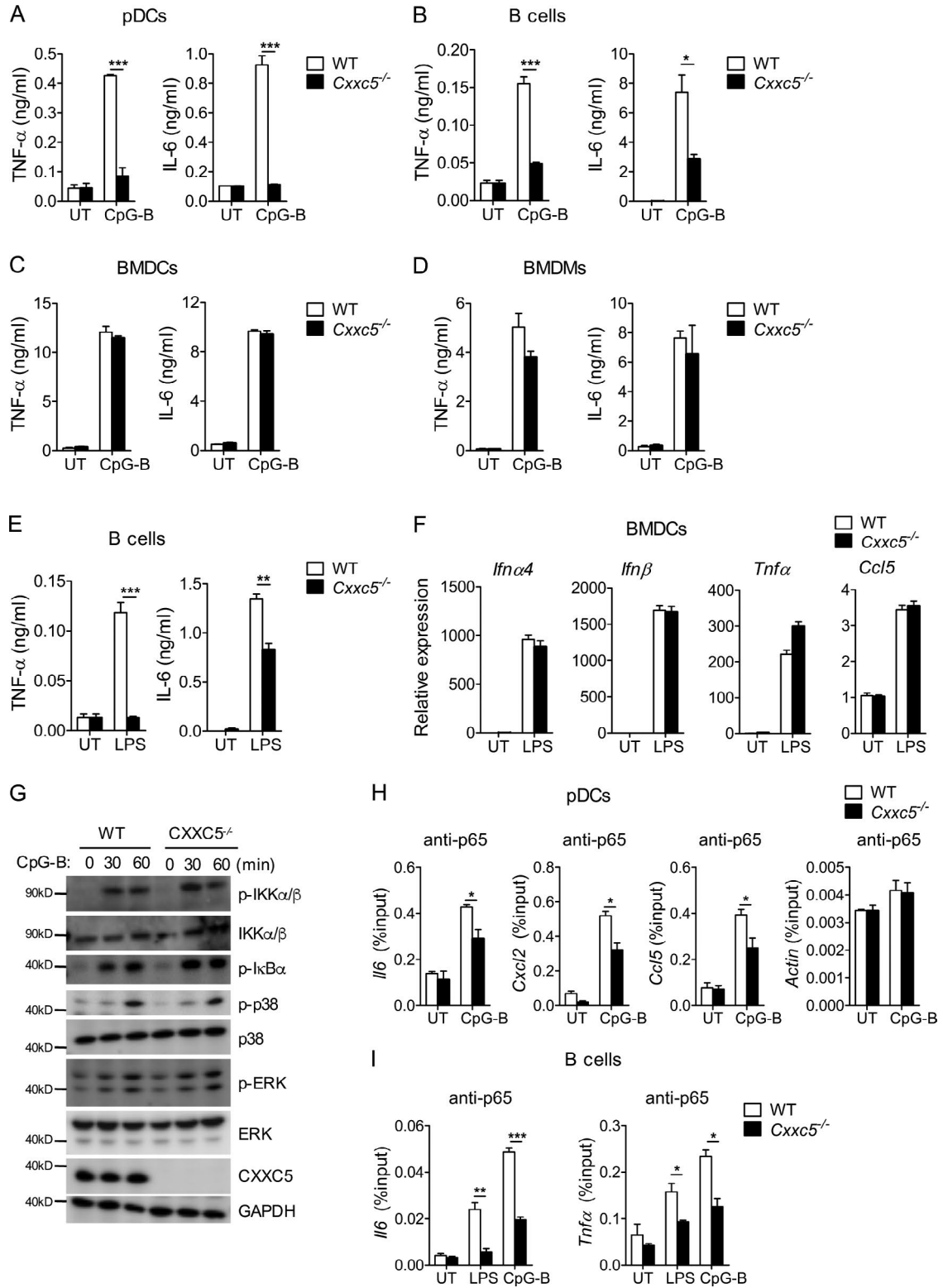


Figure 3. **Effects of CXXC5 on CpG-B- and LPS-induced signaling in various immune cell populations.** (A–D) Flt3L-pDCs ($10^6/ml$), splenic B cells ($10^7/ml$, purified by anti-CD19 microbeads), GM-CSF-BMDCs (cDCs, $10^6/ml$), and BMDMs ($10^6/ml$) were stimulated by CpG-B (100 nM) for 24 h, and supernatants ($n = 3$) were collected for ELISA. These experiments were conducted three times, and the data are presented as mean \pm SD (*, $P < 0.05$; ***, $P < 0.001$, by Student's t test). (E) Splenic B cells ($10^7/ml$) were either untreated (UT) or treated with LPS (5 $\mu g/ml$) for 48 h, and secreted cytokines were measured by ELISA. This experiment was conducted twice with similar results, and the data are presented as mean \pm SD (**, $P < 0.01$; ***, $P < 0.001$, by Student's t test). (F) BMDCs

Irf7, along with other CGI-containing genes *Fos*, *Cxcl2*, and *Tnf α* , were indeed down-regulated in steady-state CXXC5^{-/-} pDCs; however, some non-CGI genes such as *Thr7/9* and *Tcf4* (which encodes E2-2) were normally expressed in these cells (Fig. 5 B). By Western blotting, we further confirmed that the expression of IRF7 was attenuated in steady-state CXXC5^{-/-} pDCs, whereas other regulators of pDC function, such as IRF5, IRF8, and STAT3, were unaffected (Fig. 5 C). Notably, the major regulators of IFN α/β signaling, such as IFN α R1/2, STAT1/2, and IRF9, were expressed at comparable levels in both WT and CXXC5^{-/-} pDCs (Fig. 5 D).

Next, we sought to examine whether CXXC5 may exert its effect on CGI-containing genes, in particularly *Irf7*, through an epigenetic mechanism. Although CXXC5 has been shown to reside in either the cytoplasm or the nucleus, varying with cell types, we found that CXXC5 proteins were predominantly presented in the nuclei of pDCs (Fig. 6 A). By ChIP-qPCR analyses, we observed specific enrichment of CXXC5 within the CpG island located in the first intron of *Irf7* gene (500–1,000; Fig. 6 B). Moreover, bisulfate sequencing revealed that this CpG-rich region (500–1,000) was hypomethylated in the pDCs (16.25%) but hypermethylated in the cDCs (57.5%; Fig. 6, C and D). Remarkably, ablation of CXXC5 led to elevated DNA methylation in pDCs (36.25%) but not in cDCs (52.5%; Fig. 6, C and D). Conversely, the hydroxylation of 5-methyl-cytosine (5hmC), the first of three steps leading to 5mC demethylation (Xu et al., 2011), was lessened not only in *Irf7* CGI, but also in the CGIs of *Cxcl2* and *Tnf α* in CXXC5^{-/-} pDCs (Fig. 6 E). These results therefore suggested a novel role for CXXC5 in regulation of DNA methylation in pDCs.

Because CGI methylation can lead to the recruitment of chromatin remodeling complexes such as PRC2 and HDACs, we subsequently investigated whether CXXC5 is involved in the regulation of chromatin remodeling. By ChIP-qPCR, we found that Ezh2, the core component of PRC2, was highly enriched in the CGI of *Irf7* in CXXC5^{-/-} pDCs, whereas the enrichment of Sin3a was unaltered (Fig. 6 F). Moreover, the presence of H3K27me3, a repressive marker primarily assembled by histone methyltransferase Ezh2, was markedly enhanced in *Irf7* CGI of CXXC5^{-/-} pDCs (Fig. 6 G). Conversely, several active histone markers (such as H3K4me3, H3K36me3, H3K27ac, H3ac, and H4ac) were concomitantly decreased in the same CGI region of CXXC5^{-/-} pDCs (Fig. 6 G). As a result, polymerase II (pol II) binding to *Irf7* pro-

motor was impaired in CXXC5^{-/-} pDCs (Fig. 6 H). Collectively, these data implied that CXXC5 might be required for the maintenance of active chromatin structure on *Irf7*, possibly through regulating DNA methylation and histone modifications.

CXXC5 recruits Tet2 to regulate DNA methylation and *Irf7* expression

Because of a lack of enzymatic activity, it is conceivable that CXXC5 has to work with other partners to regulate DNA methylation. One of the candidate partners for CXXC5 is DNA demethylase Tet2 which, unlike Tet1 and Tet3, does not possess a CXXC domain (Xu et al., 2011, 2012; Long et al., 2013). To test this scenario, we conducted coimmunoprecipitation and identified CXXC5/Tet2 complexes in WT pDCs (Fig. 7 A). We then generated a series of mutants of CXXC5 and tested their interactions with Tet2 in HEK293T cells. Consistent with a previous studies (Ko et al., 2013), although WT CXXC5 colocalized with Tet2 in the nuclei, the CXXC domain-disrupted mutant of CXXC5 (C258A/C286A) failed to colocalize with Tet2 (Fig. S2 A). Moreover, the DNA binding domain-disrupted mutant of CXXC5 (TGHQ to AGAA) also lost the interaction with Tet2 (Fig. S2 A). Notably, ChIP-qPCR analyses revealed that Tet2 was also predominantly enriched in the 500–1,000 region within the CGI of *Irf7* gene, a process dependent on the expression of CXXC5 in pDCs (Fig. 7 B).

We then tested whether Tet2 is involved in the regulation of CGI methylation in pDCs. By bisulfate sequencing, we detected elevated DNA methylation in *Irf7* CGI of Tet2^{-/-} pDCs (Fig. 7 C), a phenomenon similarly observed in CXXC5^{-/-} pDCs (Fig. 6 C). Moreover, histone markers H3K36me3 and H3K4me3 were less enriched in *Irf7* CGI of Tet2^{-/-} pDCs (Fig. 7 D). However, unlike CXXC5, Tet2 did not seem to have an impact on the enrichment of H3K27me3 or Ezh2 in this region (Fig. 7, D and E). Consistent with these epigenetic changes, Tet2^{-/-} pDCs expressed much less IRF7 than WT controls (Fig. 7 F). Interestingly, overexpression of WT, but not Tet2 binding-deficient mutants of CXXC5, resulted in constitutive *Irf7* expression in cDCs (Fig. S2 B). Consequently, only WT, but not those mutants of CXXC5, was able to elevate *Ifn α 4* and *Ifn β* expression in cDCs after LPS stimulation (Fig. S2 C). By ELISA, we were able to detect greater IFN β production in CXXC5-overexpressing cDCs upon LPS stimulation, although IFN α remained undetectable (Fig. S2 D).

(cDCs; 10⁶/ml) were either untreated or treated with LPS (100 ng/ml) for 4 h, and the induction of *Ifn α/β* , chemokine, and cytokine mRNAs was analyzed by real-time PCR. This experiment was repeated once, and the data are presented as mean \pm SD. (G) Flt3L-differentiated pDCs from WT and CXXC5^{-/-} mice were stimulated with CpG-B (100 nM) for various times. Cell lysates were resolved by 10% SDS-PAGE and probed with the indicated antibodies. This experiment was repeated twice. (H and I) Flt3L-pDCs were stimulated with CpG-B (100 nM) for 2 h, and splenic B cells were treated with LPS (5 μ g/ml) or CpG-B (150 nM) for 2 h. After cross-linking and FACS sorting, cell lysates were prepared and immunoprecipitated with 2 μ g anti-p65. Immunoprecipitated promoters of proinflammatory genes were measured by real-time PCR and quantified over respective inputs ($n = 4$). These experiments were repeated twice, and representative data (mean \pm SD) are shown (*, $P < 0.05$; **, $P < 0.01$; ***, $P < 0.001$, analyzed by Student's t test).

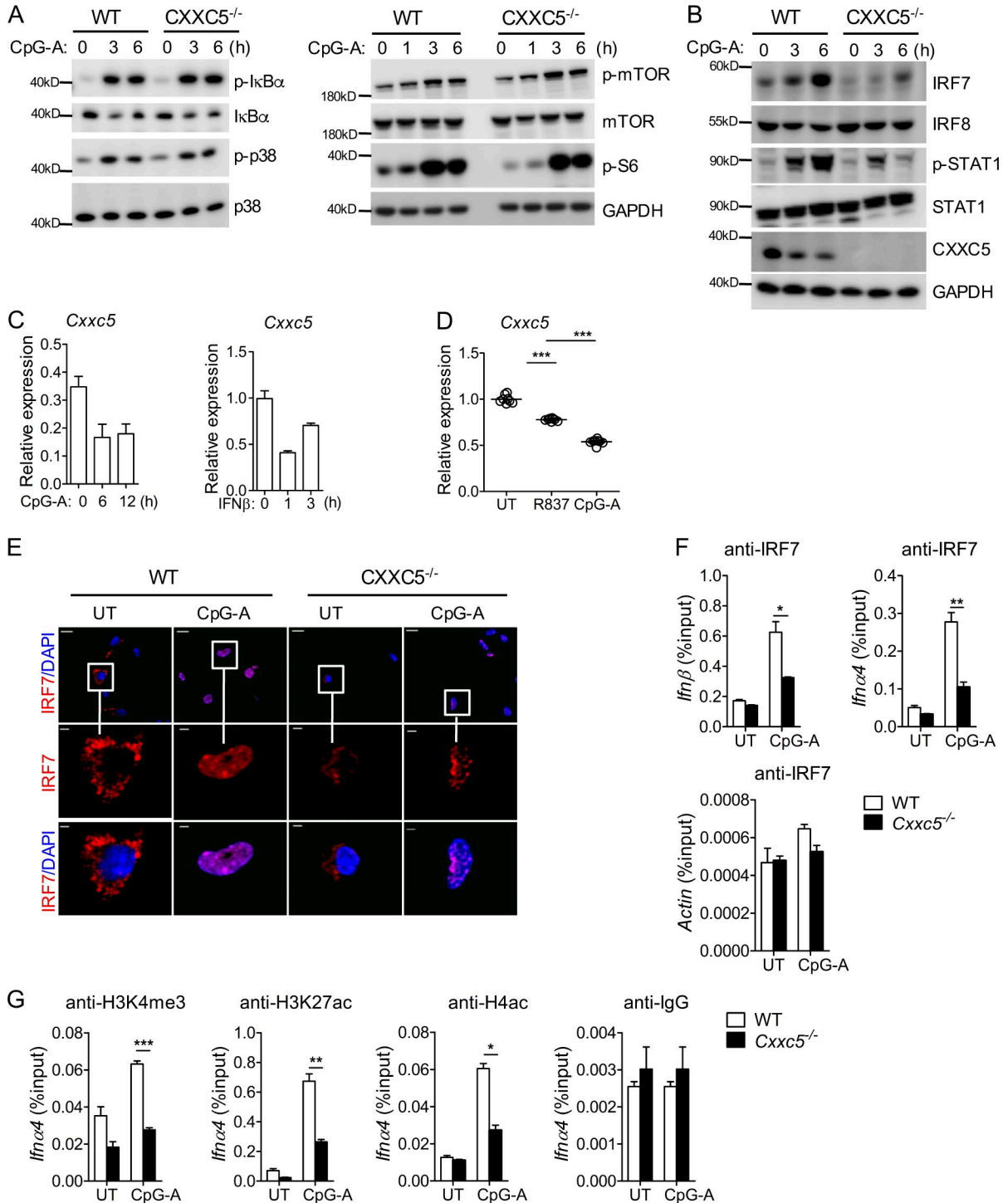


Figure 4. Impact of CXXC5 on CpG-A-induced TLR9 signaling in pDCs. (A and B) Flt3L-differentiated pDCs from WT and CXXC5^{-/-} mice were stimulated with CpG-A (2 μg/ml) for various times. Cell lysates were resolved by 10% SDS-PAGE and probed with the indicated antibodies. These experiments were repeated twice with similar results. (C and D) Flt3L-differentiated pDCs were stimulated with CpG-A (ODN1585; 2 μg/ml) or IFNβ (100 U/ml) for various times (C), and human pDCs sorted from PBMCs of eight healthy individuals were treated with R837 (20 μg/ml) or CpG-A (ODN2216; 1 μM) for 24 h (D). These experiments were repeated twice, and expression levels of *Cxhc5* were analyzed by real-time PCR (mean ± SD; ***, P < 0.001). (E) Flt3L-differentiated pDCs were either untreated (UT) or treated with CpG-A (2 μg/ml) for 5 h. Cells were fixed with paraformaldehyde and stained with anti-IRF7 antibodies (red) and DAPI (blue) sequentially. This experiment was repeated twice, and images were collected by a laser capture confocal microscope. Bars: (top) 10 μm; (bottom) 2 μm. (F and G) Flt3L-differentiated pDCs were either untreated or treated with CpG-A (2 μg/ml) for 2 h and cross-linked with paraformaldehyde.

Besides *Irf7*, we observed decreased 5hmCs in CGIs of *Cxcl2* and *Tnf α* in Tet2^{-/-} pDCs (Fig. 7 G). Moreover, pol II binding to these promoters was attenuated in Tet2^{-/-} pDCs (Fig. 7 H). Consistently, the transcription of *Irf7*, *Cxcl2*, and *Tnf α* was also impaired in Tet2^{-/-} pDCs (Fig. S2 E). These results strongly imply that CXXC5–Tet2 axis has a critical role in maintaining the hypomethylation states of a subset of CpG islands in pDCs.

CXXC5 and Tet2 play critical roles in antiviral defense

Given that CXXC5 plays a critical role in TLR7/9-induced responses in pDCs, we went on to test how this layer of regulation may contribute to host defense against viral infection in vivo. After i.v. infection by HSV-1, WT mice exhibited robust IFN response, secreting large amounts of IFN α/β and CCL-5 at the 6-h time point, whereas this early IFN response was severely impaired in CXXC5^{-/-} mice (Fig. 8 A). However, in both WT and CXXC5^{-/-} mice, the early proinflammatory responses, such as TNF and IL-12, were similarly induced after HSV-1 infection (Fig. 8 A). Moreover, the IFN response remained lower in CXXC5^{-/-} mice until 24 h after HSV-1 infection (Fig. S3 A). At that time, CXXC5^{-/-} mice exhibited ~2-log more HSV-1 viruses than WT controls (Fig. 8 B) and suffered much more severe morbidity (Fig. S3 B). By day 8, nearly 90% of CXXC5^{-/-} mice died of infection, compared with only 25% of WT mice (Fig. 8 C). Importantly, adoptively transferred WT, but not CXXC5^{-/-}, pDCs were able to alleviate the mortality of CXXC5^{-/-} mice caused by HSV-1 infection (Fig. 8 C), suggesting that the involvement of CXXC5 in pDCs might have partially contributed to host defense against HSV-1.

In addition, we found that CXXC5^{-/-} mice were also highly susceptible to VSV infection. Upon i.v. infection of VSV, CXXC5^{-/-} mice were unable to mount efficient IFN responses at the early stage of infection, exhibiting attenuated IFN α/β and CCL-5 production compared with WT mice at 6- and 24-h time points (Fig. 8 D and Fig. S3 C). Interestingly, after VSV infection, CXXC5^{-/-} mice also produced fewer IgM antibodies than WT mice on day 3, although IgG2 titers were undetectable by that time (Fig. 8 E). Furthermore, CXXC5^{-/-} mice suffered much greater weight loss than WT mice (Fig. S3 D), and eventually all died by day 5 (Fig. 8 F). In contrast, ~60% of the WT mice survived VSV infection (Fig. 8 F). Together, these results imply an indispensable role for CXXC5 in host defense against viral infection.

Considering that CXXC5 and Tet2 work in concert to regulate DNA methylation and gene expression in pDCs, we further investigated whether Tet2 has a similar role to CXXC5 in IFN response and antiviral defense. Indeed, upon stimulation by CpG-A, Tet2^{-/-} splenic pDCs produced

less IFN α and IFN β than WT controls (Fig. 9 A). After infection by HSV-1 and VSV, Tet2^{-/-} mice on mixed 129S/B6 background suffered more severe morbidity and mortality than WT mice (Fig. 9, B and C). These results suggest that Tet2 is also involved in the regulation of pDC function and antiviral defense.

CXXC5 and Tet2 regulate IFN response in human pDCs

We wondered whether CXXC5 might function similarly in human pDCs, and therefore used human pDC line Gen2.2 (Chaperot et al., 2006; Di Domizio et al., 2009) to test this scenario. We infected Gen2.2 cells with lentiviral vectors expressing scrambled or *Cxxc5*-targeted shRNAs, and then selected positive cells by GFP for further study. Interestingly, knockdown of CXXC5 led to reduced *Irf7* expression in Gen 2.2 cells (Fig. 10 A). Further, in *Cxxc5*-knockdown cells, HSV-1- and R848-induced *Ifn α* and *Ifn β* mRNAs were also impaired (Fig. 10 A). In contrast, knockdown of Tet2 also decreased *Irf7* expression and led to compromised IFN response in Gen2.2 cells (Fig. 10 B). Therefore, the CXXC5–TET2 axis might also operate in human pDCs, possibly through the same mechanism implicated in mouse pDCs (Fig. 10 C).

DISCUSSION

Despite sharing conserved molecular signatures with cDCs and B cells, pDCs are generally viewed as a key component of the innate immune system, contributing to the immediate IFN response upon viral infection. Although the signaling pathways by which TLR7/9 induces a robust IFN response have been largely defined, the involvement of epigenetic regulation in this process has yet to be established. In this study, we report that CXXC5 has a crucial role in TLR7/9-induced IFN response, and propose that DNA methylation might act as an epigenetic mechanism licensing pDC for antiviral defense.

Although CXXC5 has been previously linked to hematopoiesis and hematological malignancy (Pendino et al., 2009; Treppendahl et al., 2013), its role in the immune response has been largely unknown. Although CXXC4 is uniformly expressed in a diversity of immune cell subsets (Robbins et al., 2008; Miller et al., 2012), we and others (Robbins et al., 2008; Ghosh et al., 2010) found that CXXC5 is highly expressed in pDCs but barely detectable in cDCs or macrophages. The most notable feature distinguishing pDCs from cDCs and macrophages rests in their robust IFN-producing capacity. In this regard, we demonstrated here that ablating CXXC5 expression diminished IFN response in pDCs, whereas forcing CXXC5 expression in cDCs elevated their IFN response. Therefore, cell type-specific expression of CXXC5 seems to be one of the mechanisms underlying differential IFN-producing capacity between pDCs and cDCs. pDCs are

pDCs sorted by FACS were lysed for ChIP by anti-IRF7 (3 μ g; F) or anti-H4ac, anti-H3K4me3, and anti-H3K27ac (1 μ g; G). Immunoprecipitated *Ifn α* 4 and *Ifn β* promoter DNA fragments were measured by real-time PCR and quantified over respective inputs. These experiments were repeated twice, and data ($n = 3$, mean \pm SD) were analyzed by Student's *t* test (*, $P < 0.05$; **, $P < 0.01$; ***, $P < 0.001$).

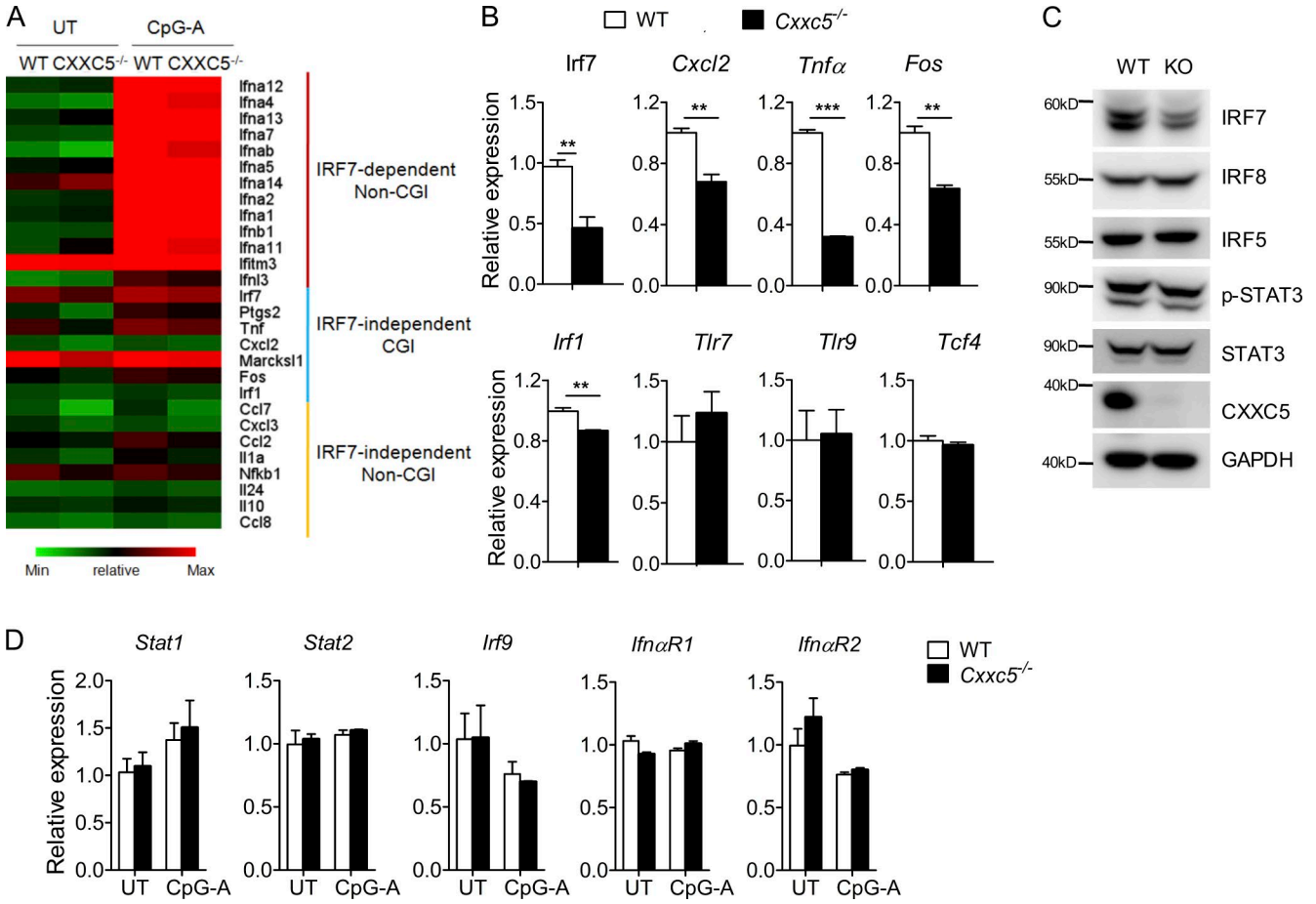


Figure 5. CXXC5-regulated gene expression in pDCs. (A) Graphic presentation of three groups of genes that were down-regulated >1.5-fold in CXXC5^{-/-} pDCs compared with WT pDCs by microarray analysis. The relative expression of each gene in four different groups is presented as log₂ value. (B) Validation of subsets of genes differentially expressed in WT and CXXC5^{-/-} pDCs by real-time PCR. This experiment was conducted twice, and data (mean ± SD) were analyzed by Student's *t* test (**, *P* < 0.01; ***, *P* < 0.001). (C) Cell lysates were prepared from Flt3L-differentiated WT and CXXC5^{-/-} (KO) pDCs, and Western blotting was conducted to detect the expression of transcriptional factors. This experiment was repeated twice with similar results. (D) Flt3-pDCs were either untreated (UT) or treated with CpG-A (2 μg/ml) for 6 h, and gene expression was analyzed by real-time PCR. This experiment was conducted twice (*n* = 3), and the data are presented as mean ± SD.

one of the major cell populations contributing to immediate IFN response against viral infection. Indeed, we found that the early IFN response, but not proinflammatory response, was diminished in CXXC5^{-/-} mice after viral infection. Interestingly, CXXC5^{-/-} mice had more pronounced virus propagation at early stages and eventually succumbed to infection. Besides pDCs, CXXC5 is modestly expressed in B cells and T cells, and thus may also have functional roles in these cells. In line with this notion, our data demonstrated that CXXC5 is involved in the regulation of TLR response and antibody production in B cells. Conceivably, all these mechanisms executed by CXXC5 might have contributed to the marked morbidity and mortality exhibited by CXXC5^{-/-} mice after HSV and VSV infection. Nevertheless, adoptive transfer of WT pDCs to CXXC5^{-/-} mice was able to ameliorate the mortality caused by HSV-1 infection, indicating an integral role for pDC in host defense. However, further studies will be

required to decipher the role of CXXC5 in other immune cells and how additional mechanisms may contribute to host defense against viral infection.

It is well known that pDCs uniquely express high levels of IRF7 at steady state, yet the underlying mechanism remains incompletely understood. Corroborating a previous study linking DNA methylation to *Irf7* silencing in human fibroblasts (Lu et al., 2000), we found that the CpG island of *Irf7* is hypermethylated in cDCs as well, suggesting that CpG methylation may be broadly involved in restriction of IRF7 expression in a variety of cells, including nonimmune and immune cells. Conversely, in pDCs, *Irf7* CGI is hypomethylated, a phenomenon that depends on the expression of both CXXC5 and Tet2. Mechanistically, our study suggests that CXXC5 may function as a “reader” for unmethylated CpGs, a scenario also implied in previous studies (Iurlaro et al., 2013; Spruijt et al., 2013), by recruiting DNA demethylase Tet2 to

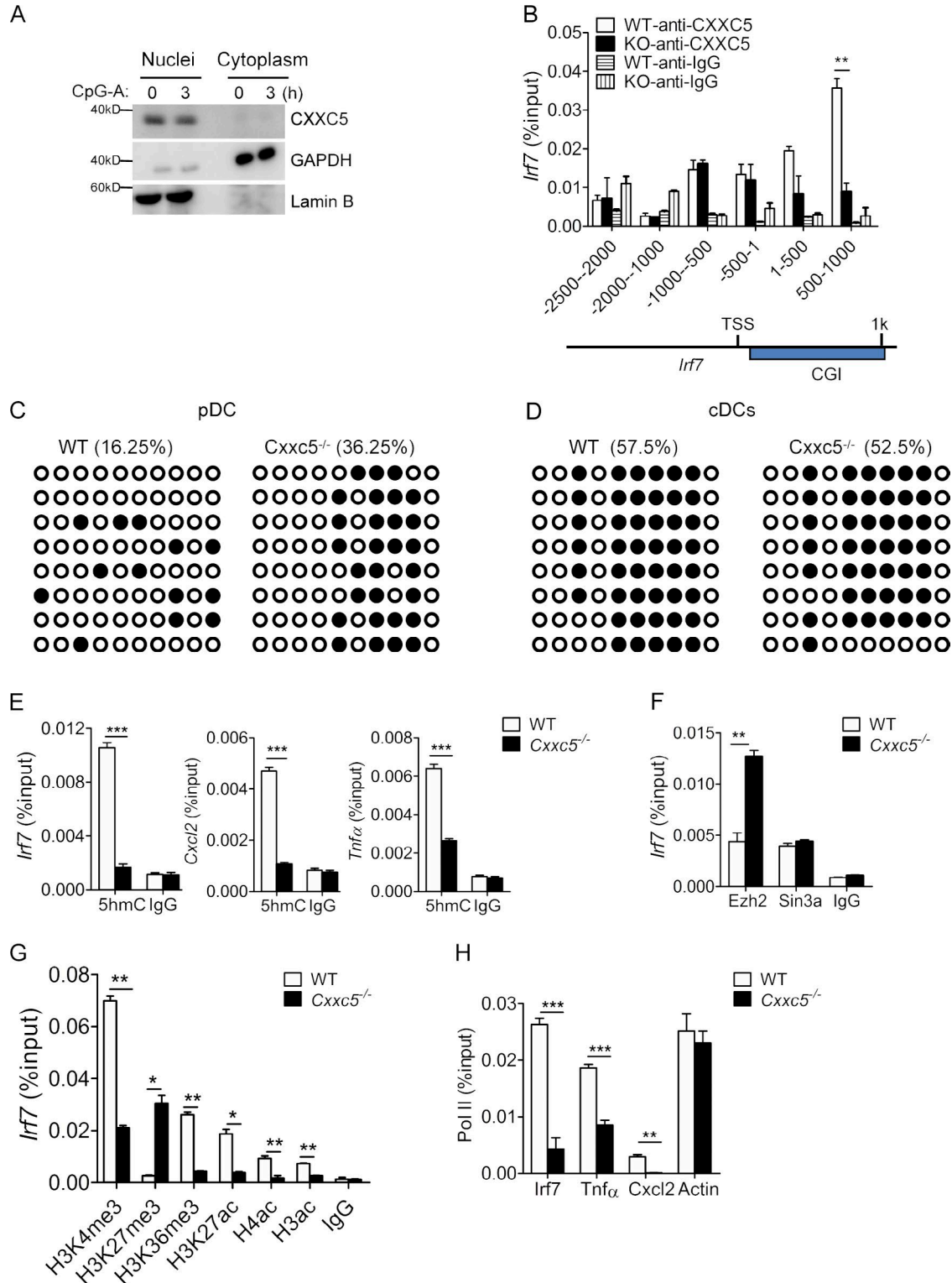


Figure 6. Epigenetic modifications on the CpG island of *Irf7* gene. (A) Flt3-pDCs were either untreated or treated with CpG-A (2 μ g/ml) for 3 h, and nuclear versus cytoplasmic distribution of CXXC5 was analyzed by Western blotting. This experiment was repeated twice with similar results. (B) Cell lysates from Flt3L-differentiated WT and *CXXC5*^{-/-} (KO) pDCs were cross-linked and immunoprecipitated with anti-CXXC5. The enrichment of various regions of *Irf7* promoter was measured by real-time PCR and quantified over respective inputs. This experiment was repeated three times, and data ($n = 4$, mean \pm SD) were analyzed by Student's *t* test (**, $P < 0.01$). TSS, transcription start site. (C and D) 500 ng genomic DNA from Flt3L-pDCs (C) and GM-CSF-cDCs (D) generated from WT and *CXXC5*^{-/-} mice were treated with sodium bisulfite, and the CGI region of *Irf7* (500–1,000) was amplified by PCR and sequenced ($n = 10$).

maintain hypomethylation of CGIs. In support of this hypothesis, *Tet2*^{-/-} mice and *CXXC5*^{-/-} mice exhibited similar defects with regard to pDC function and antiviral defense, despite their subtle difference in genetic background. However, *Tet2* can also execute physiological functions through *CXXC5*-independent mechanisms. For example, *Tet2* can be recruited to the genome through various transcriptional factors such as IκBζ (Zhang et al., 2015a), T-bet (Ichiyama et al., 2015), and Smad3/STAT5 (Yang et al., 2015), thereby participating in the induction of cytokines IL-6, IFNγ, and IL-10 in macrophages, cDCs, or T helper cells, respectively.

In addition to DNA methylation, we found that *CXXC5* can also profoundly affect histone modifications in the CGI region. It has been demonstrated that CGI-containing inflammatory genes tend to adopt “loosened” or “opened” chromatin structures, thus being poised for constitutive expression or rapid induction (Ramirez-Carrozzi et al., 2009; Kaikkonen et al., 2013; Barozzi et al., 2014). In this regard, *CXXC5*-mediated DNA hypomethylation and histone modifications may facilitate chromatin remodeling, allowing the entry of transcriptional factor E2-2 and pol II, thereby ensuring steady-state *Irf7* expression in pDCs. Potentially, this type of chromatin remodeling fueled by hypomethylated CGI may facilitate the recruitment of NFκB and pol II to a subset of proinflammatory genes, such as *Tnfα* and *Cxcl2*, as well (Fig. 10 C). Nevertheless, more studies are needed to precisely dissect the intricate interplay between DNA methylation and histone modifications in the context of gene regulation by *CXXC5*.

In addition to *Irf7*, *CXXC5* is involved in the regulation of several other CGI-containing genes, such as *Tnfα*, *Cxcl2*, and *Fos*, in steady-state pDCs. Corroborating a previous study (Ramirez-Carrozzi et al., 2009), the methylation states of these CGIs, at least for *Tnfα* and *Cxcl2*, are well correlated with their induction by TLR signals. It is likely that *CXXC5* regulates the expression of these CGI-containing genes in a direct manner, possibly via DNA demethylation. Subsequently, DNA hypomethylation may lead to active histone remodeling, thereby priming them for transcription. On the other hand, *CXXC5* may exert its effect on non-CGI genes through indirect mechanisms. One possible scenario is that some CGI-containing genes encoding transcriptional factors, such as IRF7, IRF1, and Fos, could then contribute to the induction of some non-CGI genes in activated pDCs. Although IRF7 is a well-known master regulator of IFN response, Fos and IRF1 have been widely linked to proinflammatory gene expression as well. For example, IRF1 has an indispensable role in IL-12b expression (Salkowski et al.,

1999), and Fos is involved in IL-10 induction by promoting the recruitment of NFκB to its promoter (He et al., 2015). Nevertheless, the role of *CXXC5* in immune regulation has just begun to unfold, and further studies will be required to unravel the precise mechanisms by which *CXXC5* regulates gene expression for antiviral defense.

In summary, our study not only uncovers a cell type-specific role for *CXXC5* in TLR-induced IFN type I and proinflammatory responses, but also suggests DNA methylation as a novel epigenetic mechanism integral to pDC specification and antiviral defense. Given that human *CXXC5* shows similar expression and function in pDCs, we anticipate that these findings will have further implications for viral infections and autoimmune diseases.

MATERIALS AND METHODS

Mice

CXXC5-deficient mice were generated by deleting the second exon of *Cxxc5* gene in a 129/Ola ES cell line as described in Fig. S1 A and then backcrossing onto C57BL/6 background for six generations. *Tet2*-deficient mice on mixed 129S/C57BL/6 background were generated previously (Hu et al., 2014). These mice were bred and maintained in a pathogen-free animal facility at Institut Pasteur of Shanghai. All procedures were conducted in compliance with a protocol approved by the Institutional Animal Care and Use Committee at Institut Pasteur of Shanghai.

Plasmids and reagents

Cxxc5 cDNA was amplified from C57BL/6 BM. The mutants (mutating C258/C286 to 258A/286A or TGHQ to AGAA) of *CXXC5* were constructed by overlapping PCR approach. WT and mutants of *Cxxc5* were cloned into pCDH vector by enzymes *NheI* and *EcoRI* or cloned into pIP-FLAG and pCMV vector by enzymes *BamHI* and *EcoRI* or *EcoRI* and *BamHI*, respectively.

CpG-A (ODN1585), CpG-B (ODN1826), CpG-A (ODN2216 for human), LPS, R837, and R848 were purchased from InvivoGen. Antibodies for *Tet2* (#94580), H3K4me3 (#8580), H3K27ac (#4729), H3K27me3 (#6002), and *Ezh2* (#3748) were from Abcam. Anti-*CXXC5* (I-6513-I-AP) was from Proteintech, and anti-5hmC (#39769) was from Active Motif. Antibodies against p-IκBα (#2859), p-p38 (#9211), p-JNK (#4668), JNK (#9252), p-IKKα/β, p-STAT3 (#9145), STAT3 (#9139), p-mTOR (#2971), mTOR (#2983), IRF5 (#4950), p-S6 (#4858), S6 (#2317), p-STAT1 (#7649), and STAT1 (#9172) were purchased from Cell Signaling Technology. Antibodies against ERK (SC-93), p-ERK (SC-7383),

This experiment was conducted twice. (E) Flt3L-differentiated pDCs were cross-linked and sonicated, and chromatin fragments were immunoprecipitated with 5hmC antibodies. 5hmC levels at the promoter region of *Irf7*, *Cxcl2*, and *Tnfα* were quantified by real-time PCR ($n = 3$). This experiment was repeated once, and the data are presented as mean \pm SD (**, $P < 0.001$). (F–H) Enrichment of *Ezh2* and *Sin3a* and histone modifications in *Irf7* CGI (500–1,000; F and G) and enrichment of pol II at the promoter region of *Irf7*, *Tnfα*, and *Cxcl2* (H) in pDCs were quantified by real-time PCR ($n = 3$). These experiments were repeated twice with similar results (data were analyzed by Student's *t* test and are presented as mean \pm SD; *, $P < 0.05$; **, $P < 0.01$; ***, $P < 0.001$).

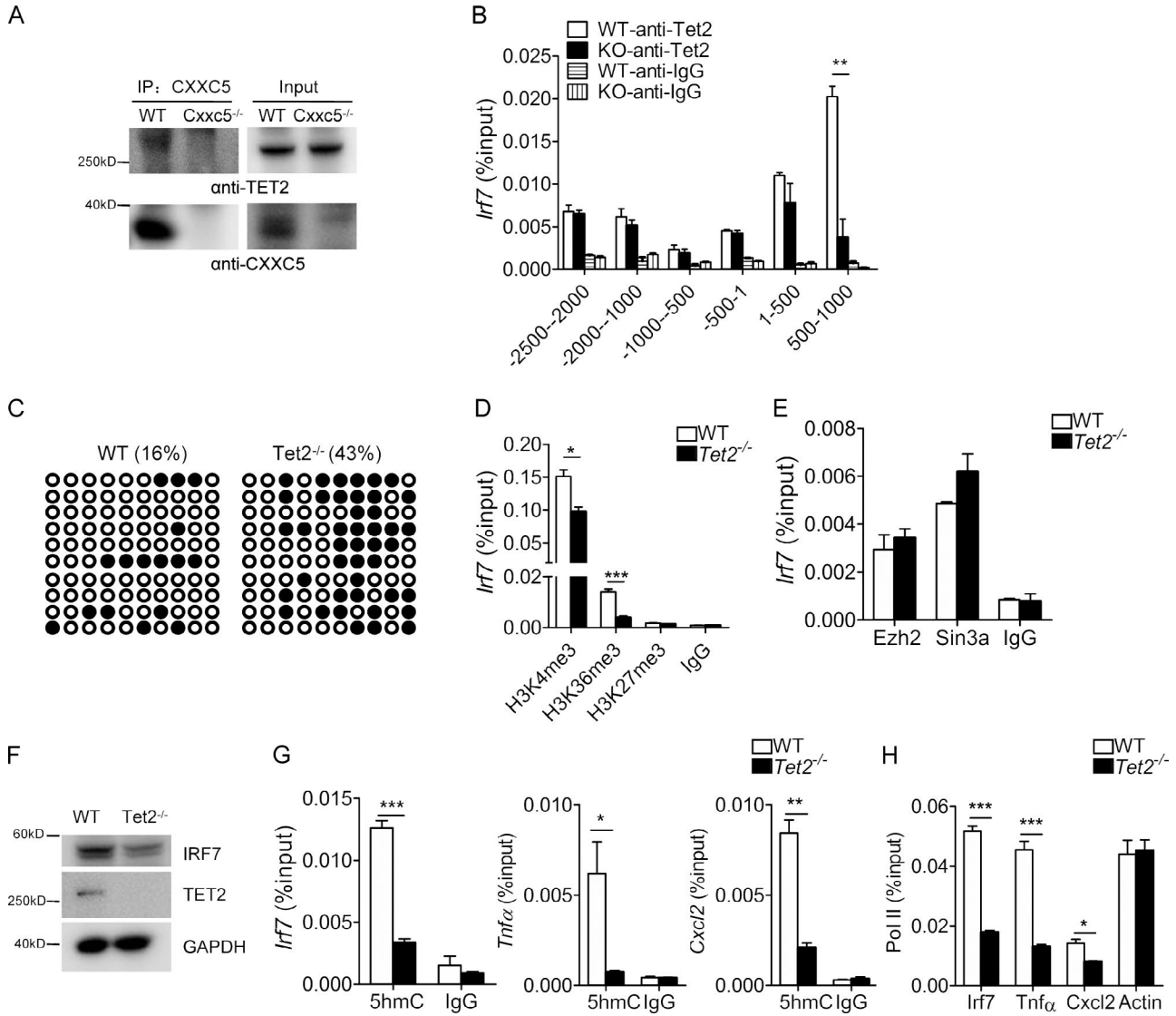


Figure 7. CXXC5 recruits Tet2 to regulate the methylation of *Irf7* CGI in pDCs. (A) Cell lysates were prepared from WT and CXXC5^{-/-} Flt3L-pDCs and immunoprecipitated (IP) with anti-CXXC5 antibody. The immunoprecipitates and inputs were blotted by anti-Tet2 and anti-CXXC5, respectively. This experiment was repeated once. (B) Whole-cell lysates from Flt3L-differentiated WT and CXXC5^{-/-} (KO) pDCs were cross-linked and immunoprecipitated by control IgG or anti-Tet2. Enrichment of Tet2 on various regions of *Irf7* promoter was determined by real-time PCR ($n = 3$). This experiment was repeated three times, and data (mean \pm SD) were analyzed by Student's *t* test (**, $P < 0.01$). (C) Genomic DNA from WT and Tet2^{-/-} Flt3L-pDCs were treated with sodium bisulfite, and the CGI region of *Irf7* (500–1,000) was amplified by PCR and sequenced ($n = 10$). This experiment was conducted twice. (D and E) Flt3L-differentiated pDCs were cross-linked and subjected to ChIP with the indicated antibodies. Histone modifications (D) and enrichment of Ezh2 and Sin3a (E) in *Irf7* CGI (500–1,000) were quantified by real-time PCR ($n = 3$). These experiments were repeated twice, and data were analyzed by Student's *t* test and are presented as mean \pm SD (*, $P < 0.05$; ***, $P < 0.001$). (F) Whole-cell lysates from Flt3L-differentiated WT and Tet2^{-/-} pDCs were resolved by 10% SDS-PAGE and probed with anti-IRF7 and anti-Tet2, respectively. This experiment was repeated once with similar results. (G and H) Flt3L-differentiated pDCs were cross-linked and sonicated, and chromatin fragments were immunoprecipitated with the indicated antibodies. 5hmC levels (G) and pol II enrichment (H) at the promoter regions of *Irf7*, *Cxcl2*, and *Tnf α* were quantified by real-time PCR ($n = 3$). These experiments were repeated twice with similar results (*, $P < 0.05$; **, $P < 0.01$; ***, $P < 0.001$, analyzed by Student's *t* test and are presented as mean \pm SD).

p38 (SC-728), Sin3a (sc-994x), I κ B α , Myc-tag, p65 (C-20), IRF8 (SC-6058), and GAPDH were from Santa Cruz Biotechnology, Inc. Anti-Flag M2 was from Sigma-Aldrich, and anti-ERK (H-72), anti-LaminB1 (332000), and anti-IRF7 (51–3300) were from Invitrogen.

Preparation of BM-derived pDCs and splenic pDCs

BM cells were isolated from femurs and tibias of 6–8-wk-old C57BL/6 mice, and red blood cells were lysed using ACK lysis buffer (0.15 M NH₄Cl, 1 mM KHCIO₃, and 0.1 mM Na₂EDTA, pH 7.3). BM cells (10⁶/ml) were seeded on

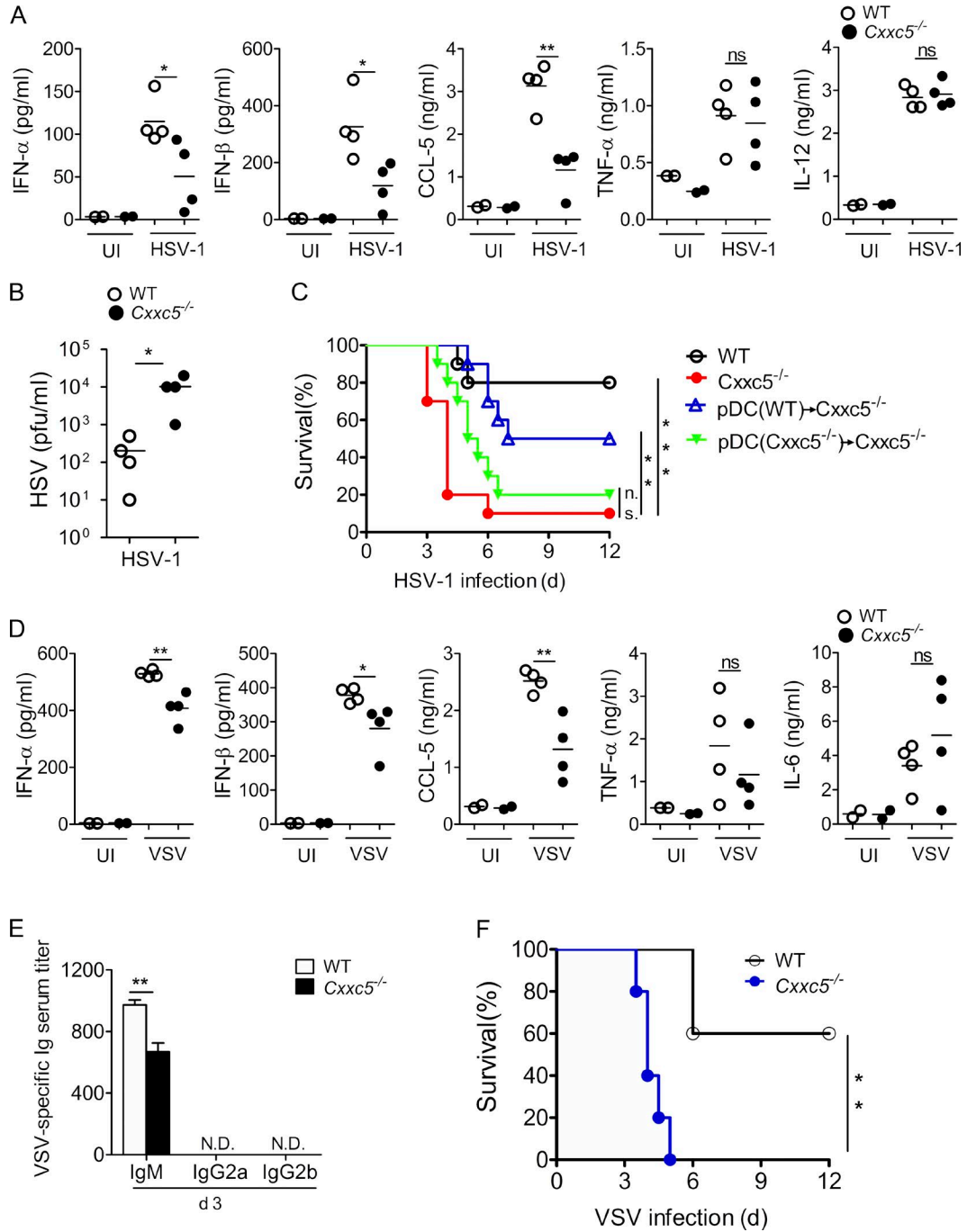


Figure 8. **CXXC5^{-/-} mice are vulnerable to viral infection in vivo.** (A and B) 6–8-wk-old WT and CXXC5^{-/-} littermates (*n* = 4) were intravenously infected with HSV-1 (5×10^6 pfu/mouse). The sera were collected at 6 h for ELISA (A) or at 24 h for plaque assay (B). These experiments were repeated three times, and data were analyzed by Student's *t* test and are presented as mean \pm SD (*, *P* < 0.05; **, *P* < 0.01; ns, not significant). (C) 6–8-wk-old WT and CXXC5^{-/-} littermates (*n* = 10) or CXXC5^{-/-} mice (*n* = 10) adoptively transferred with 1.2×10^6 Flt3L-pDCs were i.v. infected with HSV-1 (5×10^6 pfu/mouse) and monitored every 12 h for survival (**, *P* < 0.01; ***, *P* < 0.001; ns, not significant, log-rank [Mantel-Cox] test). (D–F) 6–8-wk-old WT and CXXC5^{-/-} littermates (*n* = 5) were intravenously infected with VSV (5×10^6 pfu/mouse). Sera were collected 6 h (D) or 3 d (E) after infection for ELISA, and survival was monitored every 12 h (F). These experiments were repeated once with similar results, and data were analyzed by Student's *t* test and are presented as mean \pm SD (D and E) or log-rank (Mantel-Cox) test (F; *, *P* < 0.05; **, *P* < 0.01; ns, not significant).

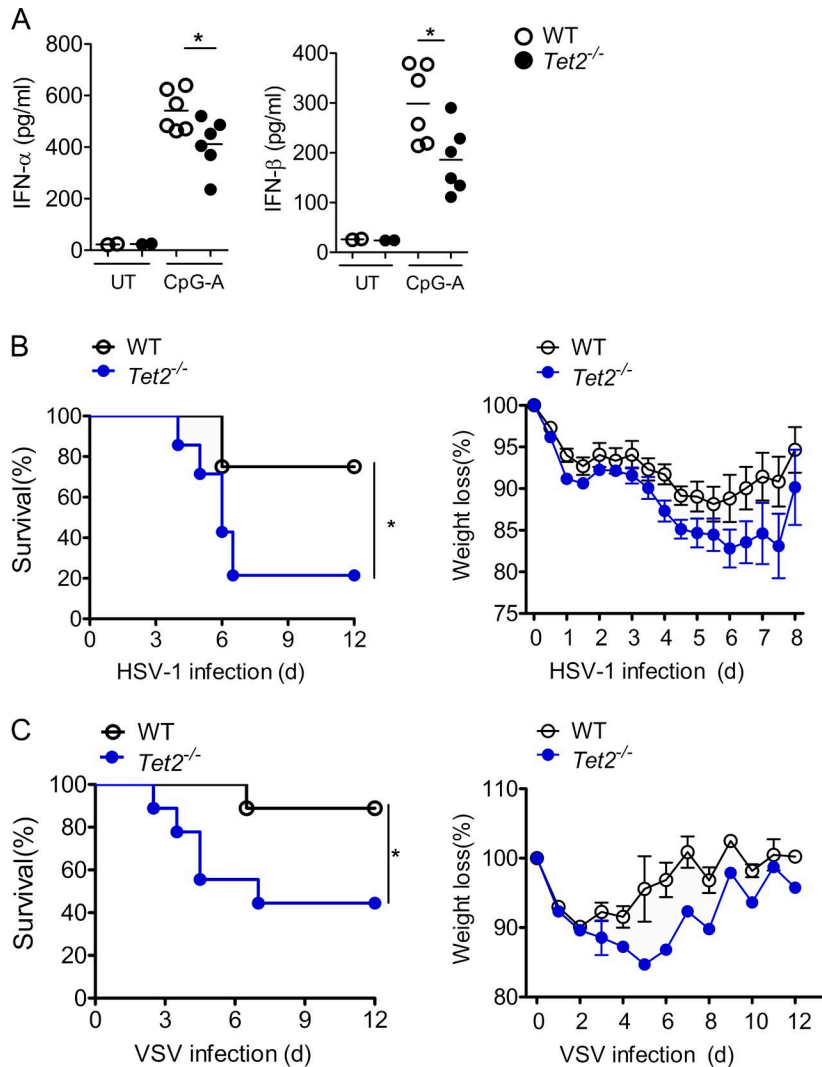


Figure 9. *Tet2*^{-/-} mice are susceptible to viral infection in vivo. (A) 10⁵ splenic pDCs sorted from WT and *Tet2*^{-/-} mice were stimulated by CpG-A (2 μ g/ml) for 48 h, and supernatants were collected for ELISA ($n = 6$). This experiment was conducted three times, and data were analyzed by Student's *t* test and are presented as mean \pm SD (*, $P < 0.05$). UT, untreated. (B) 8-wk-old WT ($n = 8$) and *Tet2*^{-/-} ($n = 14$) littermates were intravenously infected with HSV-1 (5×10^6 pfu) and monitored every 12 h for mortality and morbidity. This experiment was conducted twice, and log-rank (Mantel-Cox) test was used for statistical analysis (*, $P < 0.05$). (C) 8-wk-old WT and *Tet2*^{-/-} littermates ($n = 9$) were intravenously infected with VSV (5×10^6 pfu) and monitored every 12 h for survival and weight loss. This experiment was conducted twice, and log-rank (Mantel-Cox) test was used for statistical analysis (data are presented as mean \pm SD; *, $P < 0.05$).

RPMI 1640 medium containing 10% FBS (HyClone) and 50 ng/ml Flt3L (R&D Systems) and cultured for 5–7 d. Every 2 d, half of the media were replaced by fresh RPMI containing 10% FBS and 50 ng/ml Flt3L. Before use, suspension cells were sorted by FACS (Aria II; BD), and CD11c^{int}/B220⁺/CD11b⁻ pDCs were collected.

Splenic pDCs were prepared as described previously (Vremec et al., 2000). In brief, spleens were minced and digested with collagenase D (1 mg/ml; Sigma-Aldrich) in RPMI 1640 at 37°C for 30 min. Digested cells were passed through a nylon mesh cell strainer (BD), and incubated with anti-pDCA-1 microbeads (Miltenyi Biotec). Subsequently, enriched pDCs were labeled with CD11c, mPDCA-1, B220, and Siglec-H for FACS sorting, and the CD11c^{int}/B220⁺/mPDCA-1⁺/Siglec-H⁺ population was harvested as splenic pDCs.

Preparation of cDCs and macrophages from BM

BMDCs and BMDMs were prepared by methods described previously (Deng et al., 2015). In brief, BM cells (10^6 /ml)

were seeded on RPMI 1640 containing 10% FBS and 20 ng/ml GM-CSF (R&D Systems) and cultured for 7–9 d to generate BMDCs. BM cells (10^6 /ml) seeded on RPMI 1640 containing 10% FBS and 30% L929-conditioned medium were cultured for 5–7 d to generate BMDMs.

Antibody measurement

VSV-specific antibody titers were measured as described previously (Bach et al., 2007). In brief, 96-well plates were coated with 5 mg/ml PEG-precipitated VSV particles overnight, and then blocked with 5% BSA in PBS at RT for 2 h. Sera from uninfected and VSV-infected mice were serially diluted and incubated with precoated plates for 2 h. After extensive washing, biotin-labeled rat anti-mouse IgM, IgG2a, or IgG2b (BD) was added to detect three subtypes of antibody.

RNA preparation and real-time PCR analysis

RNAs were extracted from cultured cells or tissues using TRIzol (Invitrogen) according to the manufacturer's in-

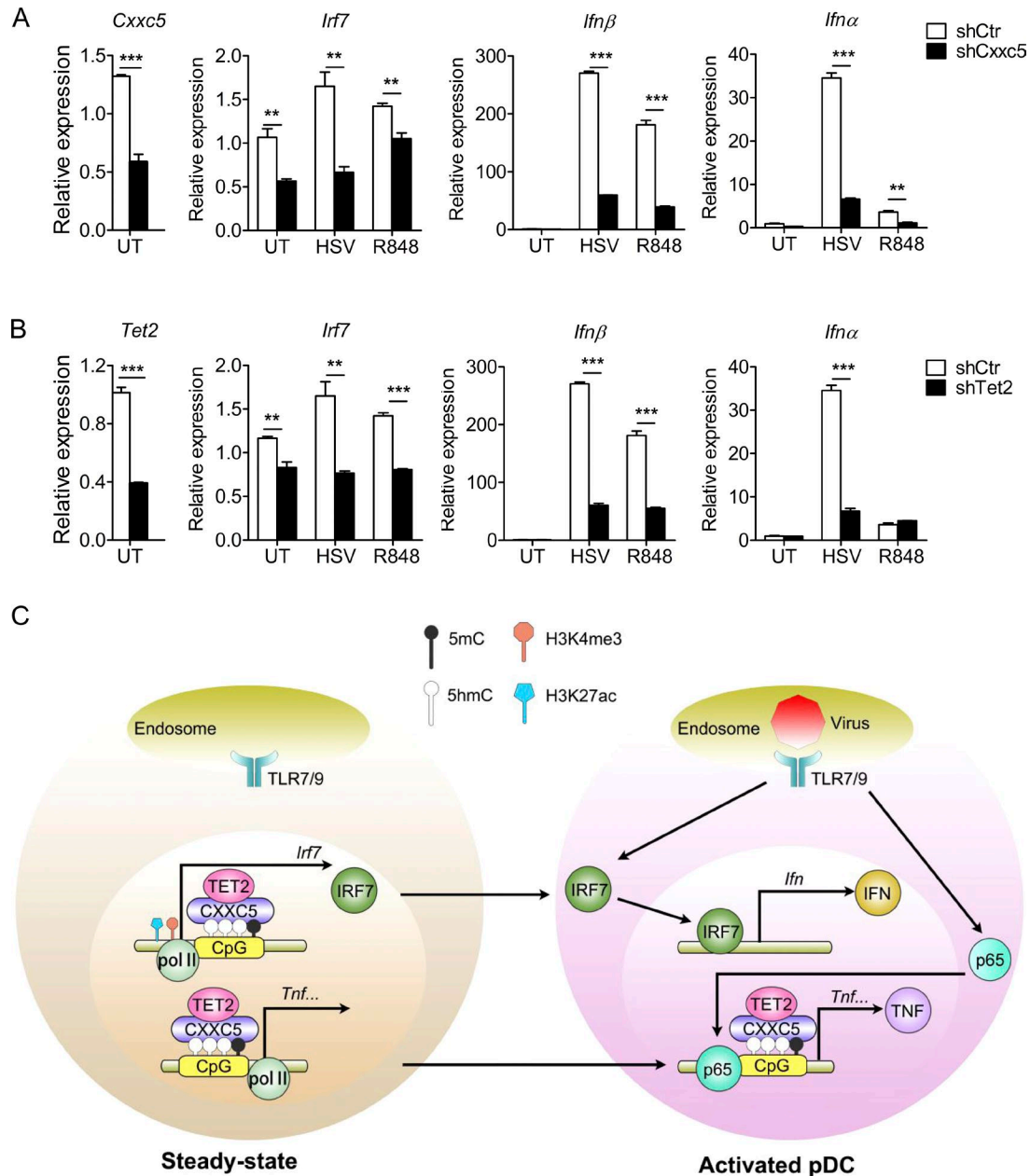


Figure 10. **CXXC5 and Tet2 regulate IFN production in human pDCs.** (A and B) Control and CXXC5- or Tet2-knockdown Gen2.2 cells were stimulated by HSV-1 (MOI: 2) or R848 (1 μ g/ml) for 4 h, and expression of *IRF7* and *IFN α / β* was analyzed by real-time PCR ($n = 4$). These experiments were repeated twice, and data shown as mean \pm SD were analyzed by Student's *t* test (**, $P < 0.01$; ***, $P < 0.001$). UT, untreated. (C) In light of our data presented here, we propose that CXXC5 may function as an epigenetic reader for hypomethylated CpG islands and work in concert with Tet2 to regulate gene expression in pDCs. By impacting DNA methylation and the ensuing histone modifications, CXXC5 not only promotes constitutive expression of the CGI-containing transcriptional factors (such as IRF7), but also opens up the proinflammatory gene promoters (such as *Tnf α*), thereby priming pDCs for TLR7/9-induced IFN and proinflammatory responses.

struction. cDNAs were reverse transcribed from 0.5 μ g total RNAs by PrimeScript RT-PCR kit (Takara Bio Inc.). Real-time PCR was performed with PrimeScript RT reagent kit (Takara Bio Inc.) on an ABI 7900HT Fast Real-time PCR System. Relative expression levels of target genes were quantitatively normalized against the expression of *GAPDH* using

the $\Delta\Delta$ CT method. All real-time PCR primers used in this study are described in Table S2.

Microarray analysis

Total mRNAs (1 μ g) were obtained from Flt3L-differentiated WT and *CXXC5*^{-/-} pDCs either untreated or treated

with 2 µg/ml CpG-A for 3 h and analyzed by Agilent Technologies Gene Expression Hybridization kit according to the manufacturer's protocols. Agilent Technologies Feature Extraction software (version 11.0.1.1) was used to analyze acquired array images. Quantitative normalization and subsequent data processing were performed with the GeneSpring GX v12.1 software package (Agilent Technologies). GEO accession no. is GSE79643.

ChIP assay

Flt3L-differentiated BM DCs were either untreated or treated with CpG-A (2 µg/ml) for 2 h before cross-linking, and FACS-sorted cells were then used for immunoprecipitation. Cells were cross-linked with 1% methanol-free formaldehyde for 10 min at room temperature. Cross-linking was quenched by 125 mM glycine for 5 min, and cell pellets were washed twice with PBS. Subsequently, cells were lysed in sonication buffer (10 mM Tris-HCl, pH 8.0, 100 mM NaCl, 1 mM EDTA, 0.5 mM EGTA, 0.1% sodium deoxycholate, and 0.5% *N*-lauroylsarcosine) at 4°C and sonicated for 22 cycles (20 s on and 50 s off per cycle) to obtain DNA fragments averaging 500 bp. Chromatins were immunoprecipitated overnight with 1–3 µg of respective antibodies and then incubated with Dynabeads Protein A or G (Invitrogen) for 2 h at 4°C. Beads containing protein–DNA complexes were washed seven times with RIPA buffer (50 mM Hepes, pH 7.5, 500 mM LiCl, 1 mM EDTA, 1% NP-40, and 0.7% sodium deoxycholate), followed by washes with 1 mM Tris-EDTA/300 mM NaCl and 1 mM Tris-EDTA/50 mM NaCl (once each). Cross-linking was reversed, and DNAs were eluted with 100 µl extraction buffer (1% SDS, 100 mM NaHCO₃, and 300 mM NaCl) by boiling for 15 min. Next, proteins were degraded with 1 mg/ml proteinase K at 55°C, and DNAs were extracted by phenol-chloroform and precipitated by ethanol. Both immunoprecipitated DNAs and input DNAs were resuspended in 100 µl 0.1× TE buffer for real-time PCR. The real-time PCR primers used for ChIP assay are listed in Table S2.

Hydroxymethylated DNA immunoprecipitation and bisulfite sequencing

Genomic DNAs were purified and fragmented by sonication to generate DNA fragments ranging from 200 to 500 bp. Sonicated DNAs (4 µg) were denatured and incubated with control IgG or anti-5hmC (0.2 µl) at 4°C overnight. Antibody–DNA complexes were captured by protein A beads preincubated with salmon sperm DNA. Immunoprecipitated DNAs were purified with a PCR purification kit and quantified by real-time PCR against input DNAs.

500 ng of genomic DNAs prepared by phenol-chloroform extraction and ethanol precipitation, and treated with RNase A for 15 min at 37°C, were used for bisulfite conversion in an EpiTech bisulfite kit (QIAGEN) according to the manufacturer's instruction. Bisulfite-sequencing primers were designed according to MethPrimer software. Specific

fragments were amplified by PCR and cloned into pMD18T vector (Takara Bio Inc.). Isolated plasmids with expected fragments were sequenced, and the methylation states were analyzed by BiqAnalyzer.

Western blotting

To make whole-cell lysates, cells were lysed in lysis buffer (50 mM Tris, pH 7.4, 150 mM NaCl, 1% Triton X-100, and 1 mM EDTA, pH 8.0) supplemented with protease inhibitor complete mini (Roche) and 1 mM PMSF, 1 mM Na₃VO₄, and 1 mM NaF for 30 min on ice, and cell debris was cleared by centrifugation at 13,000 rpm for 15 min.

To make cytosolic and nuclear extracts, cells were resuspended in hypotonic buffer (10 mM Hepes, pH 7.6, 1.5 mM MgCl₂, 10 mM KCl, and 1 mM EDTA) supplemented with protease inhibitor complete mini (Roche) and gently homogenized by Douncer (10–15 strokes). After centrifugation at 3,000 rpm for 5 min, the supernatant was removed as crude cytosolic fraction; the pellet was washed twice in hypotonic buffer and further lysed in high-salt buffer (20 mM Hepes, pH 7.6, 500 mM NaCl, 1.5 mM MgCl₂, and 1 mM EDTA) supplemented with protease inhibitors to generate crude nuclear fraction. Crude cytosolic and nuclear fractions were further centrifuged at 13,000 rpm for 15 min to remove debris, and supernatants were collected as cytosolic and nuclear fractions, respectively.

Confocal microscopy

Flt3L-differentiated pDCs were cultured on glass slides placed on 24-well tissue culture dishes (2 × 10⁵ cells/well) and stimulated with 2 µg/ml CpG-A or 100 nM CpG-B for 5 h. Cells were spun down and fixed with 4% paraformaldehyde for 10 min at room temperature. After treatment with 0.1% Triton-100 for 5 min at room temperature, cells were labeled with rabbit polyclonal anti-IRF7. For transfected HEK293T cells, mouse anti-Myc or rabbit anti-FlagM2 were used to stain attached cells overnight at 4°C. Anti-rabbit IgG Alexa Fluor 555 (Invitrogen) or/and anti-mouse IgG Alexa Fluor 488 (Invitrogen) were used as secondary antibodies. Slides were washed and mounted in Prolong Gold antifade mounting media with DAPI (Beyotime), and images were collected on a laser capture confocal microscope (FV1200, Olympus) using separate laser excitation to avoid any cross-interference between different fluorophores.

Flow cytometry

Fluorochrome-labeled antibodies for CD3 (145-2C11), CD8 (53-6.7), B220 (RA3-6B2), CD11c (N418), mPDCA1 (ebi927), Ly6C (HK1.4), and MHC-II (KH95) were from eBioscience. Antibodies for CD4 (GK1.5), Ly6G (IA8), and CD11b (M1/70) were purchased from BD. All antibodies were tested for their specificity with respective isotype controls. Cell-surface staining was performed by incubating cells with specific antibodies for 30 min on ice and washing with MACS buffer twice. All samples were processed with a

Fortessa flow cytometer (BD), and data were analyzed with FlowJo software (Tree Star).

Lentivirus preparation and transduction

Lentiviral vectors pcdh-EGFP expressing WT or mutants of CXXC5 were transiently transfected into HEK293T cells along with packaging plasmids (Δ 8.91/VSV-G), and virus-containing media were harvested in 48 h. Lentiviruses were added onto BM cells cultured with RPMI 1640 supplemented with Flt3L (50 ng/ml) or GM-CSF (20 ng/ml) on day 2. After infection for 24 h, virus-containing media were removed and substituted with pDC or BMDC differentiation media. 1 d later, GFP⁺ cells were sorted by FACS and continued in culture for 5 d.

Scrambled or Tet2- and CXXC5-specific shRNAs were subcloned into pLKO.1-EGFP vector, and lentiviral particles were prepared as described above in this section. Gen2.2 cell culture and transduction were conducted according to previous studies (Chaperot et al., 2006; Li et al., 2014). In brief, Gen2.2 cells were cultured in Gluta-Max-RPMI 1640 (Thermo Fisher Scientific) supplemented with 10% FBS/2mM L-glutamine/1 \times MEM-non-essential amino acid/1 mM sodium pyruvate and infected by shRNA-expressing lentiviral particles in the presence of 4 mg/ml polybrene (Sigma-Aldrich) for 48 h. Subsequently, lentiviral-infected GFP-positive cells were sorted with BD FACS Aria II, followed by HSV-1 and R848 stimulation.

Viral infection

6–8-wk-old and sex-matched littermates were infected i.v. with HSV-1 (KOS strain, 5×10^6 pfu) or VSV (Indiana strain, 5×10^6 pfu) in 0.1 ml PBS. Weight loss and survival were monitored every 12 h. Sera for ELISA were collected 6 h after infection, and spleens for real-time PCR analyses were taken 24 h after infection. For plaque assays, sera samples obtained 24 h after HSV-1 infection were sonicated, serially diluted, and added into confluent Vero cells cultured on 24-well plates. 1.5 h after infection, the supernatant was removed and the cells were overlaid by 2 \times MEM containing 1.6% agar. 5 d later, the overlay was removed and cells were fixed with 4% formaldehyde for 2 h and stained with 0.5% crystal violet. The plaques were counted, and viral titers were calculated accordingly.

Statistical analysis

Log-rank (Mantel–Cox) test and Student's *t* test were used for statistical analysis; *P* < 0.05 is considered significant.

Online supplemental material

Fig. S1 shows the gene-targeting strategy and immune cell development for CXXC5-deficient mice. Fig. S2 demonstrates that CXXC5 requires both CXXC and DNA-binding domains to execute its Tet2-dependent function in regulating *Irf7* and *Ifi α 4/ β* expression. Fig. S3 shows HSV- and VSV-induced splenic IFN responses and morbidity in WT and CXXC5-

deficient mice. Table S1 is a list of genes regulated by CXXC5 in pDCs. Table S2 is a list of primers used in this study.

ACKNOWLEDGMENTS

We are grateful to Prof. Gang Wei and Dr. Ying Li from Institute of Computational Biology for their assistance in ChIP assay. We are also indebted to Bangguo Qian for his technical support in confocal microscopy.

This study was supported by the Ministry of Science and Technology of the People's Republic of China Key Development and Research Project (2016YFA0502102 to H. Xiao) and National Science and Technology 973 project (2014CB541902 to H. Xiao and N. Shen), the National Natural Science Foundation of China (grants 31470847 and 91542206 to H. Xiao), and the Strategic Priority Research Program of the Chinese Academy of Sciences (grant XDB19000000).

The authors declare no competing financial interests.

Author contributions: S. Ma, Z. Deng, L. Shi, C. Hao, Z. Zhou, C. Zhou, Y. Fang, J. Liu, J. Yang, X. Chen, T. Li, and A. Zang performed experiments; X. Wan and Y. Zhang generated CXXC5-deficient mice; S. Yin and L. Jiang provided assistance on ChIP assays and microarray data analysis; B. Li, J. Plumas, L. Chaperot, X. Zhang, G.L. Xu, N. Shen, S. Xiong, and X. Gao provided materials and technical supports essential for this project; H. Xiao and S. Ma analyzed the data and wrote the paper.

Submitted: 21 July 2016

Revised: 20 January 2017

Accepted: 3 March 2017

REFERENCES

- Andersson, T., E. Södersten, J.K. Duckworth, A. Cascante, N. Fritz, P. Sacchetti, I. Cervenka, V. Bryja, and O. Hermanson. 2009. CXXC5 is a novel BMP4-regulated modulator of Wnt signaling in neural stem cells. *J. Biol. Chem.* 284:3672–3681. <http://dx.doi.org/10.1074/jbc.M808119200>
- Bach, P., E. Kamphuis, B. Odermatt, G. Sutter, C.J. Buchholz, and U. Kalinke. 2007. Vesicular stomatitis virus glycoprotein displaying retrovirus-like particles induce a type I IFN receptor-dependent switch to neutralizing IgG antibodies. *J. Immunol.* 178:5839–5847. <http://dx.doi.org/10.4049/jimmunol.178.9.5839>
- Barozzi, I., M. Simonatto, S. Bonifacio, L. Yang, R. Rohs, S. Ghisletti, and G. Natoli. 2014. Coregulation of transcription factor binding and nucleosome occupancy through DNA features of mammalian enhancers. *Mol. Cell.* 54:844–857. <http://dx.doi.org/10.1016/j.molcel.2014.04.006>
- Blackledge, N.P., and R. Klose. 2011. CpG island chromatin: A platform for gene regulation. *Epigenetics.* 6:147–152. <http://dx.doi.org/10.4161/epi.6.2.13640>
- Blackledge, N.P., J.P. Thomson, and P.J. Skene. 2013. CpG island chromatin is shaped by recruitment of ZF-CxxC proteins. *Cold Spring Harb. Perspect. Biol.* 5:a018648. <http://dx.doi.org/10.1101/cshperspect.a018648>
- Blasius, A.L., P. Krebs, B.M. Sullivan, M.B. Oldstone, and D.L. Popkin. 2012. Slc15a4, a gene required for pDC sensing of TLR ligands, is required to control persistent viral infection. *PLoS Pathog.* 8:e1002915. <http://dx.doi.org/10.1371/journal.ppat.1002915>
- Cao, W., S. Manicassamy, H. Tang, S.P. Kasturi, A. Pirani, N. Murthy, and B. Pulendran. 2008. Toll-like receptor-mediated induction of type I interferon in plasmacytoid dendritic cells requires the rapamycin-sensitive PI(3)K–mTOR–p70S6K pathway. *Nat. Immunol.* 9:1157–1164. <http://dx.doi.org/10.1038/ni.1645>
- Cervantes-Barragan, L., K.L. Lewis, S. Firner, V. Thiel, S. Hugues, W. Reith, B. Ludewig, and B. Reizis. 2012. Plasmacytoid dendritic cells control T-cell response to chronic viral infection. *Proc. Natl. Acad. Sci. USA.* 109:3012–3017. <http://dx.doi.org/10.1073/pnas.1117359109>

- Chaperot, L., A. Blum, O. Manches, G. Lui, J. Angel, J.P. Molens, and J. Plumas. 2006. Virus or TLR agonists induce TRAIL-mediated cytotoxic activity of plasmacytoid dendritic cells. *J. Immunol.* 176:248–255. <http://dx.doi.org/10.4049/jimmunol.176.1.248>
- Chehimi, J., D.E. Campbell, L. Azzoni, D. Bacheller, E. Pappasavvas, G. Jerandi, K. Mounzer, J. Kostman, G. Trinchieri, and L.J. Montaner. 2002. Persistent decreases in blood plasmacytoid dendritic cell number and function despite effective highly active antiretroviral therapy and increased blood myeloid dendritic cells in HIV-infected individuals. *J. Immunol.* 168:4796–4801. <http://dx.doi.org/10.4049/jimmunol.168.9.4796>
- Ciancanelli, M.J., S.X. Huang, P. Luthra, H. Garner, Y. Itan, S. Volpi, F.G. Lafaille, C. Trouillet, M. Schmolke, R.A. Albrecht, et al. 2015. Infectious disease. Life-threatening influenza and impaired interferon amplification in human IRF7 deficiency. *Science.* 348:448–453. <http://dx.doi.org/10.1126/science.aaa1578>
- Decalf, J., S. Fernandes, R. Longman, M. Ahloulay, F. Audat, F. Lefrerre, C.M. Rice, S. Pol, and M.L. Albert. 2007. Plasmacytoid dendritic cells initiate a complex chemokine and cytokine network and are a viable drug target in chronic HCV patients. *J. Exp. Med.* 204:2423–2437. <http://dx.doi.org/10.1084/jem.20070814>
- Deng, Z., S. Ma, H. Zhou, A. Zang, Y. Fang, T. Li, H. Shi, M. Liu, M. Du, P.R. Taylor, et al. 2015. Tyrosine phosphatase SHP-2 mediates C-type lectin receptor-induced activation of the kinase Syk and anti-fungal TH17 responses. *Nat. Immunol.* 16:642–652. <http://dx.doi.org/10.1038/ni.3155>
- Di Domizio, J., A. Blum, M. Gallagher-Gambarelli, J.P. Molens, L. Chaperot, and J. Plumas. 2009. TLR7 stimulation in human plasmacytoid dendritic cells leads to the induction of early IFN-inducible genes in the absence of type I IFN. *Blood.* 114:1794–1802. <http://dx.doi.org/10.1182/blood-2009-04-216770>
- Duan, X.Z., M. Wang, H.W. Li, H. Zhuang, D. Xu, and F.S. Wang. 2004. Decreased frequency and function of circulating plasmacytoid dendritic cells (pDC) in hepatitis B virus infected humans. *J. Clin. Immunol.* 24:637–646. <http://dx.doi.org/10.1007/s10875-004-6249-y>
- Farcas, A.M., N.P. Blackledge, I. Sudbery, H.K. Long, J.F. McGouran, N.R. Rose, S. Lee, D. Sims, A. Cerase, T.W. Sheahan, et al. 2012. KDM2B links the Polycomb Repressive Complex 1 (PRC1) to recognition of CpG islands. *eLife.* 1:e00205. <http://dx.doi.org/10.7554/eLife.00205>
- Ganguly, D., G. Chamilos, R. Lande, J. Gregorio, S. Meller, V. Facchinetti, B. Homey, E.J. Barrat, T. Zal, and M. Gilliet. 2009. Self-RNA-antimicrobial peptide complexes activate human dendritic cells through TLR7 and TLR8. *J. Exp. Med.* 206:1983–1994. <http://dx.doi.org/10.1084/jem.20090480>
- Ganguly, D., S. Haak, V. Sisirak, and B. Reizis. 2013. The role of dendritic cells in autoimmunity. *Nat. Rev. Immunol.* 13:566–577. <http://dx.doi.org/10.1038/nri3477>
- Ghosh, H.S., B. Cisse, A. Bunin, K.L. Lewis, and B. Reizis. 2010. Continuous expression of the transcription factor e2-2 maintains the cell fate of mature plasmacytoid dendritic cells. *Immunity.* 33:905–916. <http://dx.doi.org/10.1016/j.immuni.2010.11.023>
- Gu, T.P., F. Guo, H. Yang, H.P. Wu, G.F. Xu, W. Liu, Z.G. Xie, L. Shi, X. He, S.G. Jin, et al. 2011. The role of Tet3 DNA dioxygenase in epigenetic reprogramming by oocytes. *Nature.* 477:606–610. <http://dx.doi.org/10.1038/nature10443>
- He, L., A. Zang, M. Du, D. Ma, C. Yuan, C. Zhou, J. Mu, H. Shi, D. Li, X. Huang, et al. 2015. mTOR regulates TLR-induced c-fos and Th1 responses to HBV and HCV vaccines. *Viol. Sin.* 30:174–189. <http://dx.doi.org/10.1007/s12250-015-3606-3>
- Honda, K., H. Yanai, H. Negishi, M. Asagiri, M. Sato, T. Mizutani, N. Shimada, Y. Ohba, A. Takaoka, N. Yoshida, and T. Taniguchi. 2005. IRF-7 is the master regulator of type-I interferon-dependent immune responses. *Nature.* 434:772–777. <http://dx.doi.org/10.1038/nature03464>
- Hoshino, K., T. Sugiyama, M. Matsumoto, T. Tanaka, M. Saito, H. Hemmi, O. Ohara, S. Akira, and T. Kaisho. 2006. IkappaB kinase- α is critical for interferon- α production induced by Toll-like receptors 7 and 9. *Nature.* 440:949–953. <http://dx.doi.org/10.1038/nature04641>
- Hu, X., L. Zhang, S.-Q. Mao, Z. Li, J. Chen, R.-R. Zhang, H.-P. Wu, J. Gao, F. Guo, W. Liu, et al. 2014. Tet and TDG mediate DNA demethylation essential for mesenchymal-to-epithelial transition in somatic cell reprogramming. *Cell Stem Cell.* 14:512–522. <http://dx.doi.org/10.1016/j.stem.2014.01.001>
- Ichiyama, K., T. Chen, X. Wang, X. Yan, B.S. Kim, S. Tanaka, D. Ndiaye-Lobry, Y. Deng, Y. Zou, P. Zheng, et al. 2015. The methylcytosine dioxygenase Tet2 promotes DNA demethylation and activation of cytokine gene expression in T cells. *Immunity.* 42:613–626. <http://dx.doi.org/10.1016/j.immuni.2015.03.005>
- Iurlaro, M., G. Ficiz, D. Oxley, E.A. Raiber, M. Bachman, M.J. Booth, S. Andrews, S. Balasubramanian, and W. Reik. 2013. A screen for hydroxymethylcytosine and formylcytosine binding proteins suggests functions in transcription and chromatin regulation. *Genome Biol.* 14:R119. <http://dx.doi.org/10.1186/gb-2013-14-10-r119>
- Izaguirre, A., B.J. Barnes, S. Amrute, W.S. Yeow, N. Megjugorac, J. Dai, D. Feng, E. Chung, P.M. Pitha, and P. Fitzgerald-Bocarsly. 2003. Comparative analysis of IRF and IFN- α expression in human plasmacytoid and monocyte-derived dendritic cells. *J. Leukoc. Biol.* 74:1125–1138. <http://dx.doi.org/10.1189/jlb.0603255>
- Kaikkonen, M.U., N.J. Spann, S. Heinz, C.E. Romanoski, K.A. Allison, J.D. Stender, H.B. Chun, D.F. Tough, R.K. Prinjha, C. Benner, and C.K. Glass. 2013. Remodeling of the enhancer landscape during macrophage activation is coupled to enhancer transcription. *Mol. Cell.* 51:310–325. <http://dx.doi.org/10.1016/j.molcel.2013.07.010>
- Karrich, J.J., L.C.M. Jachimowski, C.H. Uittenbogaart, and B. Blom. 2014. The plasmacytoid dendritic cell as the Swiss army knife of the immune system: Molecular regulation of its multifaceted functions. *J. Immunol.* 193:5772–5778. <http://dx.doi.org/10.4049/jimmunol.1401541>
- Kawai, T., S. Sato, K.J. Ishii, C. Coban, H. Hemmi, M. Yamamoto, K. Terai, M. Matsuda, J. Inoue, S. Uematsu, et al. 2004. Interferon- α induction through Toll-like receptors involves a direct interaction of IRF7 with MyD88 and TRAF6. *Nat. Immunol.* 5:1061–1068. <http://dx.doi.org/10.1038/ni1118>
- Kawai, T., K. Takahashi, S. Sato, C. Coban, H. Kumar, H. Kato, K.J. Ishii, O. Takeuchi, and S. Akira. 2005. IPS-1, an adaptor triggering RIG-I- and Mda5-mediated type I interferon induction. *Nat. Immunol.* 6:981–988. <http://dx.doi.org/10.1038/ni1243>
- Kim, H.Y., J.Y. Yoon, J.H. Yun, K.W. Cho, S.H. Lee, Y.M. Rhee, H.S. Jung, H.J. Lim, H. Lee, J. Choi, et al. 2015. CXXC5 is a negative-feedback regulator of the Wnt/ β -catenin pathway involved in osteoblast differentiation. *Cell Death Differ.* 22:912–920. <http://dx.doi.org/10.1038/cdd.2014.238>
- Kim, M.S., S.K. Yoon, F. Bollig, J. Kitagaki, W. Hur, N.J. Whye, Y.P. Wu, M.N. Rivera, J.Y. Park, H.S. Kim, et al. 2010. A novel Wilms tumor 1 (WT1) target gene negatively regulates the WNT signaling pathway. *J. Biol. Chem.* 285:14585–14593. <http://dx.doi.org/10.1074/jbc.M109.094334>
- Kim, M.Y., H.Y. Kim, J. Hong, D. Kim, H. Lee, E. Cheong, Y. Lee, J. Roth, D.G. Kim, S. Min, and K.Y. Choi. 2016. CXXC5 plays a role as a transcription activator for myelin genes on oligodendrocyte differentiation. *Glia.* 64:350–362. <http://dx.doi.org/10.1002/glia.22932>
- Ko, M., J. An, H.S. Bandukwala, L. Chavez, T. Aijö, W.A. Pastor, M.F. Segal, H. Li, K.P. Koh, H. Lähdesmäki, et al. 2013. Modulation of TET2 expression and 5-methylcytosine oxidation by the CXXC domain protein IDAX. *Nature.* 497:122–126. <http://dx.doi.org/10.1038/nature12052>
- Ko, M., J. An, W.A. Pastor, S.B. Koralov, K. Rajewsky, and A. Rao. 2015. TET proteins and 5-methylcytosine oxidation in hematological cancers. *Immunol. Rev.* 263:6–21. <http://dx.doi.org/10.1111/imr.12239>
- Lande, R., J. Gregorio, V. Facchinetti, B. Chatterjee, Y.H. Wang, B. Homey, W. Cao, Y.H. Wang, B. Su, F.O. Nestle, et al. 2007. Plasmacytoid dendritic

- cells sense self-DNA coupled with antimicrobial peptide. *Nature*. 449:564–569. <http://dx.doi.org/10.1038/nature06116>
- Laouar, Y., T. Welte, X.Y. Fu, and R.A. Flavell. 2003. STAT3 is required for Flt3L-dependent dendritic cell differentiation. *Immunity*. 19:903–912. [http://dx.doi.org/10.1016/S1074-7613\(03\)00332-7](http://dx.doi.org/10.1016/S1074-7613(03)00332-7)
- Lee, S.H., M.Y. Kim, H.Y. Kim, Y.M. Lee, H. Kim, K.A. Nam, M.R. Roh, S. Min, K.Y. Chung, and K.Y. Choi. 2015. The Dishevelled-binding protein CXXC5 negatively regulates cutaneous wound healing. *J. Exp. Med.* 212:1061–1080. <http://dx.doi.org/10.1084/jem.20141601>
- Lewis, K.L., and B. Reizis. 2012. Dendritic cells: Arbiters of immunity and immunological tolerance. *Cold Spring Harb. Perspect. Biol.* 4:a007401. <http://dx.doi.org/10.1101/cshperspect.a007401>
- Li, E., and Y. Zhang. 2014. DNA methylation in mammals. *Cold Spring Harb. Perspect. Biol.* 6:a019133. <http://dx.doi.org/10.1101/cshperspect.a019133>
- Li, G., M. Cheng, J. Nunoya, L. Cheng, H. Guo, H. Yu, Y.J. Liu, L. Su, and L. Zhang. 2014. Plasmacytoid dendritic cells suppress HIV-1 replication but contribute to HIV-1 induced immunopathogenesis in humanized mice. *PLoS Pathog.* 10:e1004291. <http://dx.doi.org/10.1371/journal.ppat.1004291>
- Li, H.S., C.Y. Yang, K.C. Nallaparaju, H. Zhang, Y.J. Liu, A.W. Goldrath, and S.S. Watowich. 2012. The signal transducers STAT5 and STAT3 control expression of Id2 and E2-2 during dendritic cell development. *Blood*. 120:4363–4373. <http://dx.doi.org/10.1182/blood-2012-07-441311>
- Long, H.K., N.P. Blackledge, and R.J. Klose. 2013. ZF-CxxC domain-containing proteins, CpG islands and the chromatin connection. *Biochem. Soc. Trans.* 41:727–740. <http://dx.doi.org/10.1042/BST20130028>
- Lu, R., W.C. Au, W.S. Yeow, N. Hageman, and P.M. Pitha. 2000. Regulation of the promoter activity of interferon regulatory factor-7 gene. Activation by interferon and silencing by hypermethylation. *J. Biol. Chem.* 275:31805–31812. <http://dx.doi.org/10.1074/jbc.M005288200>
- Lund, J.M., M.M. Linehan, N. Iijima, and A. Iwasaki. 2006. Cutting edge: Plasmacytoid dendritic cells provide innate immune protection against mucosal viral infection in situ. *J. Immunol.* 177:7510–7514. <http://dx.doi.org/10.4049/jimmunol.177.11.7510>
- Merad, M., P. Sathe, J. Helft, J. Miller, and A. Mortha. 2013. The dendritic cell lineage: ontogeny and function of dendritic cells and their subsets in the steady state and the inflamed setting. *Annu. Rev. Immunol.* 31:563–604. <http://dx.doi.org/10.1146/annurev-immunol-020711-074950>
- Mildner, A., and S. Jung. 2014. Development and function of dendritic cell subsets. *Immunity*. 40:642–656. <http://dx.doi.org/10.1016/j.immuni.2014.04.016>
- Miller, J.C., B.D. Brown, T. Shay, E.L. Gautier, V. Jovic, A. Cohain, G. Pandey, M. Leboeuf, K.G. Elpek, J. Helft, et al. Immunological Genome Consortium. 2012. Deciphering the transcriptional network of the dendritic cell lineage. *Nat. Immunol.* 13:888–899. <http://dx.doi.org/10.1038/ni.2370>
- Ng, C.T., L.M. Snell, D.G. Brooks, and M.B.A. Oldstone. 2013. Networking at the level of host immunity: Immune cell interactions during persistent viral infections. *Cell Host Microbe*. 13:652–664. <http://dx.doi.org/10.1016/j.chom.2013.05.014>
- Ning, S., J.S. Pagano, and G.N. Barber. 2011. IRF7: Activation, regulation, modification and function. *Genes Immun.* 12:399–414. <http://dx.doi.org/10.1038/gene.2011.21>
- Pendino, F., E. Nguyen, I. Jonassen, B. Dysvik, A. Azouz, M. Lanotte, E. Ségal-Bendirdjian, and J.R. Lillehaug. 2009. Functional involvement of RINF, retinoid-inducible nuclear factor (CXXC5), in normal and tumoral human myelopoiesis. *Blood*. 113:3172–3181. <http://dx.doi.org/10.1182/blood-2008-07-170035>
- Ramirez-Carrozzi, V.R., D. Braas, D.M. Bhatt, C.S. Cheng, C. Hong, K.R. Doty, J.C. Black, A. Hoffmann, M. Carey, and S.T. Smale. 2009. A unifying model for the selective regulation of inducible transcription by CpG islands and nucleosome remodeling. *Cell*. 138:114–128. <http://dx.doi.org/10.1016/j.cell.2009.04.020>
- Reizis, B., A. Bunin, H.S. Ghosh, K.L. Lewis, and V. Sisirak. 2011a. Plasmacytoid dendritic cells: Recent progress and open questions. *Annu. Rev. Immunol.* 29:163–183. <http://dx.doi.org/10.1146/annurev-immunol-031210-101345>
- Reizis, B., M. Colonna, G. Trinchieri, F. Barrat, and M. Gilliet. 2011b. Plasmacytoid dendritic cells: One-trick ponies or workhorses of the immune system? *Nat. Rev. Immunol.* 11:558–565. <http://dx.doi.org/10.1038/nri3027>
- Robbins, S.H., T. Walzer, D. Dembélé, C. Thibault, A. Defays, G. Bessou, H. Xu, E. Vivier, M. Sellars, P. Pierre, et al. 2008. Novel insights into the relationships between dendritic cell subsets in human and mouse revealed by genome-wide expression profiling. *Genome Biol.* 9:R17. <http://dx.doi.org/10.1186/gb-2008-9-1-r17>
- Rowland, S.L., J.M. Riggs, S. Gilfillan, M. Bugatti, W. Vermi, R. Kolbeck, E.R. Unanue, M.A. Sanjuan, and M. Colonna. 2014. Early, transient depletion of plasmacytoid dendritic cells ameliorates autoimmunity in a lupus model. *J. Exp. Med.* 211:1977–1991. <http://dx.doi.org/10.1084/jem.20132620>
- Salkowski, C.A., K. Kopydlowski, J. Blanco, M.J. Cody, R. McNally, and S.N. Vogel. 1999. IL-12 is dysregulated in macrophages from IRF-1 and IRF-2 knockout mice. *J. Immunol.* 163:1529–1536.
- Sato, M., H. Suemori, N. Hata, M. Asagiri, K. Ogasawara, K. Nakao, T. Nakaya, M. Katsuki, S. Noguchi, N. Tanaka, and T. Taniguchi. 2000. Distinct and essential roles of transcription factors IRF-3 and IRF-7 in response to viruses for IFN- α/β gene induction. *Immunity*. 13:539–548. [http://dx.doi.org/10.1016/S1074-7613\(00\)00053-4](http://dx.doi.org/10.1016/S1074-7613(00)00053-4)
- Sisirak, V., D. Ganguly, K.L. Lewis, C. Couillault, L. Tanaka, S. Bolland, V. D'Agati, K.B. Elkon, and B. Reizis. 2014. Genetic evidence for the role of plasmacytoid dendritic cells in systemic lupus erythematosus. *J. Exp. Med.* 211:1969–1976. <http://dx.doi.org/10.1084/jem.20132522>
- Smale, S.T., A. Tarakhovskiy, and G. Natoli. 2014. Chromatin contributions to the regulation of innate immunity. *Annu. Rev. Immunol.* 32:489–511. <http://dx.doi.org/10.1146/annurev-immunol-031210-101303>
- Smit, J.J., B.D. Rudd, and N.W. Lukacs. 2006. Plasmacytoid dendritic cells inhibit pulmonary immunopathology and promote clearance of respiratory syncytial virus. *J. Exp. Med.* 203:1153–1159. <http://dx.doi.org/10.1084/jem.20052359>
- Spruijt, C.G., F. Gnerlich, A.H. Smits, T. Pfaffeneder, P.W. Jansen, C. Bauer, M. Münzel, M. Wagner, M. Müller, F. Khan, et al. 2013. Dynamic readers for 5-(hydroxy)methylcytosine and its oxidized derivatives. *Cell*. 152:1146–1159. <http://dx.doi.org/10.1016/j.cell.2013.02.004>
- Swiecki, M., and M. Colonna. 2015. The multifaceted biology of plasmacytoid dendritic cells. *Nat. Rev. Immunol.* 15:471–485. <http://dx.doi.org/10.1038/nri3865>
- Swiecki, M., S. Gilfillan, W. Vermi, Y. Wang, and M. Colonna. 2010. Plasmacytoid dendritic cell ablation impacts early interferon responses and antiviral NK and CD8(+) T cell accrual. *Immunity*. 33:955–966. <http://dx.doi.org/10.1016/j.immuni.2010.11.020>
- Swiecki, M., Y. Wang, S. Gilfillan, and M. Colonna. 2013. Plasmacytoid dendritic cells contribute to systemic but not local antiviral responses to HSV infections. *PLoS Pathog.* 9:e1003728. <http://dx.doi.org/10.1371/journal.ppat.1003728>
- Takagi, H., T. Fukaya, K. Eizumi, Y. Sato, K. Sato, A. Shibasaki, H. Otsuka, A. Hijikata, T. Watanabe, O. Ohara, et al. 2011. Plasmacytoid dendritic cells are crucial for the initiation of inflammation and T cell immunity in vivo. *Immunity*. 35:958–971. <http://dx.doi.org/10.1016/j.immuni.2011.01.014>
- Treppendahl, M.B., L. Möllgård, E. Hellström-Lindberg, P. Cloos, and K. Grønbaek. 2013. Downregulation but lack of promoter hypermethylation or somatic mutations of the potential tumor suppressor CXXC5 in

- MDS and AML with deletion 5q. *Eur. J. Haematol.* 90:259–260. <http://dx.doi.org/10.1111/ejh.12045>
- Tsuchiya, Y., T. Naito, M. Tenno, M. Maruyama, H. Koseki, I. Taniuchi, and Y. Naoe. 2016. ThPOK represses CXXC5, which induces methylation of histone H3 lysine 9 in Cd40lg promoter by association with SUV39H1: Implications in repression of CD40L expression in CD8⁺ cytotoxic T cells. *J. Leukoc. Biol.* 100:327–338. <http://dx.doi.org/10.1189/jlb.1A0915-396RR>
- Vremec, D., J. Pooley, H. Hochrein, L. Wu, and K. Shortman. 2000. CD4 and CD8 expression by dendritic cell subtypes in mouse thymus and spleen. *J. Immunol.* 164:2978–2986. <http://dx.doi.org/10.4049/jimmunol.164.6.2978>
- Webster, B., S. Assil, M. Dreux. 2016. Cell-cell sensing of viral infection by plasmacytoid dendritic cells. *J. Virol.* 90:10050–10053. <http://dx.doi.org/10.1128/JVI.01692-16>
- Xu, Y., F. Wu, L. Tan, L. Kong, L. Xiong, J. Deng, A.J. Barbera, L. Zheng, H. Zhang, S. Huang, et al. 2011. Genome-wide regulation of 5hmC, 5mC, and gene expression by Tet1 hydroxylase in mouse embryonic stem cells. *Mol. Cell.* 42:451–464. <http://dx.doi.org/10.1016/j.molcel.2011.04.005>
- Xu, Y., C. Xu, A. Kato, W. Tempel, J.G. Abreu, C. Bian, Y. Hu, D. Hu, B. Zhao, T. Cerovina, et al. 2012. Tet3 CXXC domain and dioxygenase activity cooperatively regulate key genes for *Xenopus* eye and neural development. *Cell.* 151:1200–1213. <http://dx.doi.org/10.1016/j.cell.2012.11.014>
- Yang, R., C. Qu, Y. Zhou, J.E. Konkel, S. Shi, Y. Liu, C. Chen, S. Liu, D. Liu, Y. Chen, et al. 2015. Hydrogen sulfide promotes Tet1- and Tet2-mediated Foxp3 demethylation to drive regulatory T cell differentiation and maintain immune homeostasis. *Immunity.* 43:251–263. <http://dx.doi.org/10.1016/j.immuni.2015.07.017>
- Zhang, M., R. Wang, Y. Wang, F. Diao, F. Lu, D. Gao, D. Chen, Z. Zhai, and H. Shu. 2009. The CXXC finger 5 protein is required for DNA damage-induced p53 activation. *Sci. China C Life Sci.* 52:528–538. <http://dx.doi.org/10.1007/s11427-009-0083-7>
- Zhang, Q., K. Zhao, Q. Shen, Y. Han, Y. Gu, X. Li, D. Zhao, Y. Liu, C. Wang, X. Zhang, et al. 2015a. Tet2 is required to resolve inflammation by recruiting Hdac2 to specifically repress IL-6. *Nature.* 525:389–393. <http://dx.doi.org/10.1038/nature15252>
- Zhang, Z., L. Cheng, J. Zhao, G. Li, L. Zhang, W. Chen, W. Nie, N.J. Reszka-Blanco, F.-S. Wang, and L. Su. 2015b. Plasmacytoid dendritic cells promote HIV-1-induced group 3 innate lymphoid cell depletion. *J. Clin. Invest.* 125:3692–3703. <http://dx.doi.org/10.1172/JCI82124>